

# Towards optimal space-time discretizations for reachable sets of nonlinear control systems

Janosch Rieger and Kyria Wawryk

## Abstract

Reachable sets of nonlinear control systems can in general only be approximated numerically, and these approximations are typically very expensive to compute. In this paper, we explore strategies for choosing the temporal and spatial discretizations of Euler’s method for reachable set computation in a non-uniform way to improve the performance of the method.

**Mathematics Subject Classification:** 93B03, 65L12.

**Keywords:** Reachable sets; Discretization of control systems; Numerical approximation; Euler’s method.

## 1 Introduction

The reachable set of a control system is the set of all states the system can be steered into at a given time. Reachable sets are particularly interesting in applications where they support decision-making, see e.g. [16, 25], where the controls, among other things, model time-varying external disturbances that need to be taken into account or mitigated, see e.g. [18, 24, 27], or where the reachable set models a spatial object to be controlled, see e.g. [12, 13]. Since explicit formulas for reachable sets are usually not available, these sets have to be approximated by numerical methods.

Numerical methods for the approximation of reachable sets are computationally expensive. They evolve an entire set according to a flow that is multivalued at every point in time and space, and because of the wrapping effect, a very fine spatial discretization is required to achieve a tolerable global error. In addition, tools for complexity reduction like a posteriori error estimation and step-size control are not available in this context. Currently, the only measure of quality for the approximate reachable sets at our disposal is the a priori error bound.

The convex reachable sets of linear control systems can be approximated by polytopes, and they interact with the flow of the system in a relatively straightforward way. For this reason, several algorithms have been developed in this setting, which are theoretically sound and perform well in practice, see [3, 17, 34] for efficient computations in zonotope representation, see [6, 7] for methods based on the Pontryagin maximum principle, and see [35] for an application of Benson’s algorithm.

In the context of nonlinear control systems, it is less obvious how the reachable sets can be discretized and evolved most efficiently. For this reason, there are several schools of thought that advance their ideas independently.

Since the numerical methods for linear systems are so successful, it is a natural idea to apply them to local linearizations of nonlinear systems. This results in an overapproximation of the reachable set by a collection of simple shapes on which the linearization errors are tolerable, see e.g. [1, 2, 32]. These algorithms are reported to perform very well when the system is only mildly nonlinear, and to have difficulties in the presence of strong nonlinearity, see the discussion in [32]. In recent work, this problem was addressed by introducing a nonconvex generalization of zonotopes that better conforms with nonlinear dynamics, see [22].

Another major class of numerical methods for nonlinear systems is inspired by Runge-Kutta methods for nonlinear differential equations. Some work focuses on explicit time discretizations and their properties in the absence of spatial discretization, see e.g. [8, 14, 15, 19, 33, 37]. Implicit methods, which are preferable in the context of stiff systems, were investigated in [11, 26, 29]. When implemented, the often very high computational complexity of these Runge-Kutta-type methods is mainly due to their spatial discretization in terms of grids, see e.g. [10, 23, 31].

The algorithm proposed in [9] was a first attempt to reduce the computational complexity of Euler’s method by eliminating spatial discretizations of the reachable set in intermediate time-steps, and this approach was later refined in [28]. The speedup achieved by these methods is significant, but they are not guaranteed to converge. A different, provably convergent algorithm proposed in [30] essentially reduces the problem by two dimensions by tracking only the boundary of the reachable set and using lower-dimensional information on the vector field.

In this paper, we pursue a different approach to reducing the complexity of Euler’s method in the spirit of a posteriori error analysis and adaptive refinement, which is also vaguely related to an idea that has been examined

in the context of controller synthesis, see [39]. Instead of working with uniform temporal and spatial discretizations, which is the standard approach, we explore what can be achieved by varying a non-uniform temporal grid and different spatial meshes at different temporal nodes. Since a posteriori errors are difficult to measure, we determine a non-uniform space-time discretization such that the *a priori error* is below a given error tolerance, and such that the complexity of Euler’s method applied to the nonlinear system with this particular discretization is near-optimal. The key challenge is to estimate this complexity, and then use the estimate in such a way that the resulting algorithm is provably convergent.

We proceed as follows: After introducing some background and notation in Section 2, we extend the global error analysis from [10] to non-uniform space-time discretizations in Section 3. In Sections 4.1 and 4.2, we propose two greedy algorithms – one that is similar to adaptive quadrature and one that gathers and exploits information on the reachable set – to determine efficient space-time discretizations, and we prove that for any prescribed global error tolerance, they both compute an approximate reachable set with the specified error in finite time. The numerical experiments in Section 5 show that both methods have the potential to outperform Euler’s method with uniform discretization, in particular when the control dynamics are non-stiff.

## 2 Notation

We consider the space  $\mathbb{R}^d$  equipped with the max norm  $\|\cdot\|_\infty$  and denote

$$\begin{aligned}\mathbb{R}_+^d &:= \{x \in \mathbb{R}^d : x_i \geq 0 \text{ for } i = 1, \dots, d\}, \\ \mathbb{R}_{>0}^d &:= \{x \in \mathbb{R}^d : x_i > 0 \text{ for } i = 1, \dots, d\}.\end{aligned}$$

For  $r > 0$  and  $x \in \mathbb{R}^d$ , we define the ball of radius  $r$  by

$$B_r(x) := \{y \in \mathbb{R}^d : \|x - y\|_\infty \leq r\}.$$

Let  $\mathcal{K}(\mathbb{R}^d)$  denote the collection of all nonempty and compact subsets of  $\mathbb{R}^d$ , and let  $\mathcal{KC}(\mathbb{R}^d)$  denote the collection of all nonempty, compact and convex subsets of  $\mathbb{R}^d$ . For any  $A, B \in \mathcal{K}(\mathbb{R}^d)$  and  $r \in \mathbb{R}$ , we define the operations

$$A + B = \{a + b : a \in A, b \in B\} \quad \text{and} \quad rA = \{ra : a \in A\},$$

and the Hausdorff semi-distance and distance are given by

$$\begin{aligned}\text{dist}(A, B) &= \sup_{a \in A} \inf_{b \in B} \|a - b\|_\infty, \\ \text{dist}_H(A, B) &= \max\{\text{dist}(A, B), \text{dist}(B, A)\}.\end{aligned}$$

The Hausdorff semi-distance satisfies the triangle inequality

$$\text{dist}(A, C) \leq \text{dist}(A, B) + \text{dist}(B, C) \quad \forall A, B, C \in \mathcal{K}(\mathbb{R}^d).$$

The mapping

$$\text{proj} : \mathbb{R}^d \times \mathcal{K}(\mathbb{R}^d) \rightarrow \mathbb{R}^d, \quad \text{proj}(x, A) := \text{argmin}_{a \in A} \|a - x\|,$$

is well-defined and single-valued. A set-valued function  $F : \mathbb{R}^d \rightarrow \mathcal{K}(\mathbb{R}^d)$  is called  $L$ -Lipschitz for some constant  $L \geq 0$  if we have

$$\text{dist}_H(F(x), F(y)) \leq L\|x - y\|_\infty \quad \forall x, y \in \mathbb{R}^d.$$

For any  $\rho > 0$ , we define the projector  $\pi_\rho : \mathcal{K}(\mathbb{R}^d) \rightarrow 2^{\rho\mathbb{Z}^d} \cap \mathcal{K}(\mathbb{R}^d)$  from the space  $\mathcal{K}(\mathbb{R}^d)$  to the space  $2^{\rho\mathbb{Z}^d} \cap \mathcal{K}(\mathbb{R}^d)$  of all nonempty bounded subsets of the grid  $\rho\mathbb{Z}^d$  by

$$\pi_\rho(A) := (A + B_{\frac{\rho}{2}}(0)) \cap \rho\mathbb{Z}^d.$$

It is easy to see that  $\pi_\rho(A)$  is indeed nonempty for all  $A \in \mathcal{K}(\mathbb{R}^d)$  and that

$$\text{dist}_H(A, \pi_\rho(A)) \leq \frac{\rho}{2} \quad \forall A \in \mathcal{K}(\mathbb{R}^d). \quad (1)$$

For any set  $A \subset \rho\mathbb{Z}^d$ , we denote the number of elements in  $A$  by  $\#A$ . Finally, we write

$$[m, n] = \{m, m+1, \dots, n-1, n\} \subset \mathbb{N}$$

when it is clear that the quantities in question are natural numbers, and for every  $h \in \mathbb{R}^n$ , we define the vector  $\Sigma_+ h \in \mathbb{R}^{n+1}$  of cumulative sums of  $h$  by

$$(\Sigma_+ h)_k = \sum_{j=1}^k h_j \quad \forall k \in [0, n].$$

The vector  $t := \Sigma_+ h \in \mathbb{R}^{n+1}$ , which is indexed from 0 to  $n$ , will represent the nodes of a non-uniform temporal discretization with step-sizes  $h_1, \dots, h_n$ .

### 3 Euler's method with non-uniform discretization

Throughout this paper, we consider the differential inclusion

$$\dot{x}(t) \in F(x(t)) \text{ for almost every } t \in (0, T), \quad x(0) \in X_0, \quad (2)$$

where  $X_0 \in \mathcal{K}(\mathbb{R}^d)$  and  $F : \mathbb{R}^d \rightarrow \mathcal{KC}(\mathbb{R}^d)$  is  $L$ -Lipschitz and satisfies the uniform bound

$$\sup_{x \in \mathbb{R}^d} \sup_{f \in F(x)} \|f\|_\infty \leq P. \quad (3)$$

The set

$$S^F(T) := \{x(\cdot) \in W^{1,1}([0, T], \mathbb{R}^d) : x(\cdot) \text{ solves inclusion (2)}\}$$

of absolutely continuous solutions to inclusion (2) gives rise to the reachable sets

$$R^F(t) := \{x(t) : x(\cdot) \in S^F(T)\} \quad \forall t \in [0, T].$$

Since  $X_0 \in \mathcal{K}(\mathbb{R}^d)$ , and because of the properties of the mapping  $F$ , it follows from [36, Corollary 4.5] that  $R^F(t) \in \mathcal{K}(\mathbb{R}^d)$  for all  $t \in [0, T]$ .

We approximate the solution set and the reachable sets of inclusion (2) by a fully discrete Euler scheme: Throughout this section, we fix a natural number  $n \in [1, \infty)$ , a vector  $h \in \mathbb{R}_{>0}^n$  so that  $t = \Sigma_+ h$  has  $t_n = T$ , and a vector  $\rho \in \mathbb{R}_+^{n+1}$ , and we define a set of discrete trajectories

$$S_{h,\rho}^F(T) = \{(y_k)_{k=0}^n \subset \mathbb{R}^d : y_0 \in \pi_{\rho_0}(X_0), \\ y_{k+1} \in \pi_{\rho_{k+1}}(y_k + h_{k+1}F(y_k)) \quad \forall k \in [0, n-1]\},$$

as well as the discrete reachable sets

$$R_{h,\rho}^F(k) = \{y_k : y \in S_{h,\rho}^F(T)\}.$$

Since  $X_0 \in \mathcal{K}(\mathbb{R}^d)$ , it follows directly from the properties of the mapping  $F$  and the projector  $\pi_\rho$  that  $R_{h,\rho}^F(k) \in 2^{\rho \mathbb{Z}^d} \cap \mathcal{K}(\mathbb{R}^d)$  for all  $k \in [0, n]$ . Algorithm 1 computes these approximate reachable sets without computing individual trajectories. It also computes empirical volumes of the reachable sets  $R_{h,\rho}^F(0), \dots, R_{h,\rho}^F(n)$ , and empirical average volumes of the multivalued images of  $F$  over these reachable sets. These estimated quantities will be used by Algorithm 4, see Remark 4.5 for details.

We provide a convergence theorem for this non-uniform numerical scheme.

---

**Algorithm 1:** Euler scheme for given discretization  $(h, t, \rho)$ 


---

**Input:** Discretization parameters  $h \in \mathbb{R}_{>0}^n$ ,  $t \in \mathbb{R}_{>0}^{n+1}$  and  $\rho \in \mathbb{R}_{>0}^{n+1}$

**Output:** Approximate reachable sets  $R_{h,\rho}^F(0), \dots, R_{h,\rho}^F(n) \subset \rho_k \mathbb{Z}^d$ ,

Empirical volumes  $(R_k)_{k=0}^n \in \mathbb{R}_{>0}^{n+1}$ ,

Empirical average volumes  $(F_k)_{k=0}^n \in \mathbb{R}_{>0}^{n+1}$ .

```

1  $R_{h,\rho}^F(0) \leftarrow \pi_{\rho_0}(X_0);$ 
2  $R_0 \leftarrow (\#R_{h,\rho}^F(0))\rho_0^d;$ 
3 for  $k \leftarrow 1$  to  $n$  do
4    $R_{h,\rho}^F(k) \leftarrow \emptyset;$ 
5    $F_{k-1} \leftarrow 0;$ 
6   for  $x \in R_{h,\rho}^F(k-1)$  do
7      $R_{h,\rho}^F(k) \leftarrow R_{h,\rho}^F(k) \cup \pi_{\rho_k}(x + h_k F(x));$ 
8      $F_{k-1} \leftarrow F_{k-1} + (\#\pi_{\rho_k}(x + h_k F(x)));$ 
9    $R_k \leftarrow (\#R_{h,\rho}^F(k))\rho_k^d;$ 
10   $F_{k-1} \leftarrow \frac{\rho_k^d}{h_k^d} \frac{F_{k-1}}{\#R_{h,\rho}^F(k-1)};$ 
11  $F_n \leftarrow F_{n-1};$ 

```

---

**Proposition 3.1.** For every  $y \in S_{h,\rho}^F(T)$ , there exists  $x(\cdot) \in S^F(T)$  with

$$\|y_k - x(t_k)\|_\infty \leq \frac{\rho_0}{2} e^{Lt_k} + \sum_{\ell=1}^k e^{L(t_k - t_\ell)} (e^{Lh_\ell} - 1) \left( Ph_\ell + \frac{\rho_\ell}{2} + \frac{\rho_\ell}{2Lh_\ell} \right) \quad (4)$$

for all  $k \in [0, n]$ .

*Proof.* Take any solution  $y \in S_{h,\rho}^F(T)$ , and consider the continuous linear spline  $y(\cdot) \in W^{1,1}([0, T], \mathbb{R}^d)$  given by

$$y(s) := \begin{cases} y_0, & s = 0, \\ y_k + \frac{s - t_k}{t_{k+1} - t_k} (y_{k+1} - y_k), & s \in (t_k, t_{k+1}], \quad k \in [0, n-1]. \end{cases}$$

In the following, we estimate the residual of the absolutely continuous function  $y(\cdot)$  in the inclusion (2) and invoke the Gronwall-Fillipov theorem, which guarantees the existence of a solution to inclusion (2) close to  $y(\cdot)$ .

Since  $y_0 = \pi_{\rho_0}(x_0)$  for some  $x_0 \in X_0$ , estimate (1) yields

$$\|y_0 - x_0\|_\infty \leq \frac{\rho_0}{2}. \quad (5)$$

Now fix any  $k \in [0, n-1]$ . There exists  $f \in F(y_k)$  with

$$y_{k+1} \in \pi_{\rho_{k+1}}(y_k + h_{k+1}f),$$

and estimate (1) yields

$$\begin{aligned} \|\dot{y}(s) - f\|_\infty &= \left\| \frac{1}{h_{k+1}}(y_{k+1} - y_k) - f \right\|_\infty \\ &= \frac{1}{h_{k+1}} \|y_{k+1} - (y_k + h_{k+1}f)\|_\infty \leq \frac{\rho_{k+1}}{2h_{k+1}} \quad \forall s \in (t_k, t_{k+1}). \end{aligned} \quad (6)$$

In particular, we have

$$\|\dot{y}(s)\|_\infty \leq \|f\|_\infty + \|\dot{y}(s) - f\|_\infty \leq P + \frac{\rho_{k+1}}{2h_{k+1}} \quad \forall s \in (t_k, t_{k+1}),$$

and hence

$$\begin{aligned} \|y(s) - y(t_k)\|_\infty &= \left\| \int_{t_k}^s \dot{y}(\tau) d\tau \right\|_\infty \leq \int_{t_k}^s \|\dot{y}(\tau)\|_\infty d\tau \\ &\leq \int_{t_k}^{t_{k+1}} \left( P + \frac{\rho_{k+1}}{2h_{k+1}} \right) d\tau = Ph_{k+1} + \frac{\rho_{k+1}}{2} \quad \forall s \in (t_k, t_{k+1}). \end{aligned} \quad (7)$$

It follows from inequalities (6) and (7) and the Lipschitz property of  $F$  that

$$\begin{aligned} \text{dist}(\dot{y}(s), F(y(s))) &\leq \text{dist}(\dot{y}(s), F(y(t_k))) + \text{dist}(F(y(t_k)), F(y(s))) \\ &\leq \|\dot{y}(s) - f\|_\infty + L\|y(t_k) - y(s)\|_\infty \\ &\leq \frac{\rho_{k+1}}{2h_{k+1}} + LPh_{k+1} + L\frac{\rho_{k+1}}{2} \quad \forall s \in (t_k, t_{k+1}). \end{aligned} \quad (8)$$

Because of estimates (5) and (8), the Gronwall-Filippov theorem [4, Theorem 2.4.1] yields the existence of a solution  $x(\cdot) \in S^F(T)$  that satisfies

$$\begin{aligned} \|y_k - x(t_k)\|_\infty &= \|y(t_k) - x(t_k)\|_\infty \\ &\leq \frac{\rho_0}{2} e^{Lt_k} + \sum_{\ell=1}^k \int_{t_{\ell-1}}^{t_\ell} e^{L(t_k-s)} \left( \frac{\rho_\ell}{2h_\ell} + LPh_\ell + L\frac{\rho_\ell}{2} \right) ds \\ &= \frac{\rho_0}{2} e^{Lt_k} + \sum_{\ell=1}^k e^{L(t_k-t_\ell)} \left( e^{Lh_\ell} - 1 \right) \left( \frac{\rho_\ell}{2Lh_\ell} + Ph_\ell + \frac{\rho_\ell}{2} \right) \end{aligned}$$

for all  $k \in [0, n]$ . □

The proof of the following proposition is considerably simpler than that of the corresponding result [10, Theorem 2]. Instead of constructing the Euler trajectory by elementary means, it uses the measurability of the projection mapping. This technique is in principle well-known and frequently used in the context of partial differential inclusions, see e.g. [20].

**Proposition 3.2.** *For every  $x(\cdot) \in S^F(T)$ , there exists  $y \in S_{h,\rho}^F(T)$  with*

$$\|x(t_k) - y_k\|_\infty \leq \frac{\rho_0}{2} \prod_{j=1}^k (1 + Lh_j) + \sum_{\ell=1}^k \left( \frac{\rho_\ell}{2} + \frac{LP}{2} h_\ell^2 \right) \prod_{j=\ell+1}^k (1 + Lh_j) \quad (9)$$

for all  $k \in [0, n]$ .

*Proof.* Let  $x(\cdot) \in S^F(T)$ . We prove the desired statement by induction on  $k$ . Choose any  $y_0 \in \pi_{\rho_0}(x(0))$ . Then  $y_0 \in \pi_{\rho_0}(X_0)$ , and  $y_0$  satisfies estimate (9) for  $k = 0$ .

Now assume that for some integer  $k \in [0, n-1]$ , a finite sequence  $(y_j)_{j=0}^k$  satisfying estimate (9) for all  $j \in [0, k]$  and

$$y_{j+1} \in \pi_{\rho_{j+1}}(y_j + h_{j+1}F(y_j)) \quad \forall j \in [0, k-1]$$

has been constructed. By [5, Corollary 8.2.13], the function

$$\xi(\cdot) : [t_k, t_{k+1}] \rightarrow \mathbb{R}^d, \quad \xi(s) := \text{proj}(\dot{x}(s), F(y_k)),$$

is measurable, and since  $F(y_k) \in \mathcal{KC}(\mathbb{R}^d)$ , we have  $\xi \in L^\infty([t_k, t_{k+1}], \mathbb{R}^d)$ . By [38, Theorem I.6.13], we have

$$f := \frac{1}{h_{k+1}} \int_{t_k}^{t_{k+1}} \xi(s) ds \in F(y_k).$$

Using the definition of  $\xi(\cdot)$ , the Lipschitz property of  $F$  and the bound (3), we obtain

$$\begin{aligned} \|\dot{x}(s) - \xi(s)\|_\infty &= \text{dist}(\dot{x}(s), F(y_k)) \leq \text{dist}(F(x(s)), F(y_k)) \\ &\leq L\|x(s) - y_k\|_\infty \leq L\|x(s) - x(t_k)\|_\infty + L\|x(t_k) - y_k\|_\infty \\ &\leq LP(s - t_k) + L\|x(t_k) - y_k\|_\infty, \end{aligned}$$



and we compute

$$\begin{aligned}
& \|x(t_{k+1}) - (y_k + h_{k+1}f)\|_\infty \\
&= \|(x(t_k) + \int_{t_k}^{t_{k+1}} \dot{x}(s)ds) - (y_k + \int_{t_k}^{t_{k+1}} \xi(s)ds)\|_\infty \\
&\leq \|x(t_k) - y_k\|_\infty + \int_{t_k}^{t_{k+1}} \|\dot{x}(s) - \xi(s)\|_\infty ds \\
&\leq (1 + Lh_{k+1})\|x(t_k) - y_k\|_\infty + \frac{1}{2}LP h_{k+1}^2.
\end{aligned}$$

We choose any

$$y_{k+1} \in \pi_{\rho_{j+1}}(y_k + h_{k+1}f)$$

and find that

$$\|x(t_{k+1}) - y_{k+1}\|_\infty \leq (1 + Lh_{k+1})\|x(t_k) - y_k\|_\infty + \frac{1}{2}LP h_{k+1}^2 + \frac{1}{2}\rho_{k+1}. \quad (10)$$

Using estimate (9) for  $k$  in inequality (10) yields estimate (9) for  $k + 1$ .  $\square$

All in all, we proved the following error bound for the discrete reachable sets in terms of the symmetric Hausdorff distance.

**Theorem 3.3.** *The exact and approximate reachable sets satisfy*

$$\begin{aligned}
& \text{dist}_H(R^F(t_k), R_{h,\rho}^F(k)) \\
& \leq \frac{\rho_0}{2}e^{Lt_k} + \sum_{\ell=1}^k e^{L(t_k-t_\ell)}(e^{Lh_\ell} - 1)(Ph_\ell + \frac{\rho_\ell}{2} + \frac{\rho_\ell}{2Lh_\ell})
\end{aligned} \quad (11)$$

for all  $k \in [0, n]$ .

*Proof.* The bounds given in Propositions 3.1 and 3.2 in terms of individual trajectories extend to the corresponding reachable sets. Since

$$(1 + Lh_j) \leq e^{Lh_j} \quad \text{and} \quad Lh_j \leq e^{Lh_j} - 1 \quad \forall j \in [1, n],$$

the bound in inequality (4) is larger than the bound in inequality (9).  $\square$

This error bound coincides with the bound e.g. from [10] in the special case of uniform discretizations.

---

**Algorithm 2:** Euler scheme with optimal uniform discretization

---

**Input:** Error tolerance  $\varepsilon > 0$

**Output:** Number of steps  $n$ ,

Discretization  $(h, t, \rho) \in \mathbb{R}_{>0}^n \times \mathbb{R}_{>0}^{n+1} \times \mathbb{R}_{>0}^{n+1}$ ,

Reachable sets  $R_{h^{(m)}, \rho^{(m)}}^F(k) \subset \rho_k^{(m)} \mathbb{Z}^d$ ,  $k = 0, \dots, n$

**1**  $n = \min\{m \in \mathbb{N} : m^2 \varepsilon - m(e^{LT} - 1)(PT + \frac{T}{2L}) - T^2(e^{LT} - \frac{1}{2}) \geq 0\};$

**2**  $h = \frac{T}{n} \mathbb{1}_{\mathbb{R}^n}$ ,  $t = \Sigma_+ h$ ,  $\rho = \frac{T^2}{n^2} \mathbb{1}_{\mathbb{R}^{n+1}};$

**3**  $(R_{h, \rho}^F, \sim, \sim) \leftarrow [\text{Algorithm 1}](h, t, \rho);$

---

## 4 Efficient space-time discretization

In the past, Algorithm 1 has usually been carried out with the coarsest uniform discretization

$$h_i = T/n, \quad i \in [1, n], \quad \text{and} \quad \rho_i = (T/n)^2, \quad i \in [0, n], \quad (12)$$

such that the error bound (11) with  $k = n$  satisfies the desired tolerance, see Algorithm 2. This is theoretically satisfactory, but gives away the opportunity to invest computational complexity only where it has a meaningful effect. Ideally, we would like to determine a discretization

$$(h, t, \rho) \in \mathbb{R}^n \times \mathbb{R}^{n+1} \times \mathbb{R}^{n+1}$$

such that the error bound (11) is below a given threshold and the corresponding complexity of Algorithm 1 is minimized. However, since the complexity depends on the shape, size and location of the a priori unknown reachable sets, it seems to be impossible to specify a formula for the complexity of Algorithm 1 that does not require explicit knowledge of its output.

As a consequence, we propose Algorithms 3 and 4, which generate sub-optimal, but efficient discretizations by adaptively refining the temporal and spatial meshes. We prove in Sections 4.1 and 4.2 that both algorithms terminate in finite time with a tolerable a priori error and show in Section 5 that they have the potential to outperform Algorithm 2.

To quantify the effect of mesh refinements, we decompose the approximation error

$$E(h, t, \rho) = \sum_{j=0}^n \mathcal{E}_j(h, t, \rho) \quad (13)$$

from Theorem 3.3 into the components

$$\mathcal{E}_j(h, t, \rho) := \begin{cases} e^{LT \frac{\rho_0}{2}}, & j = 0, \\ e^{L(T-t_j)}(e^{Lh_j} - 1) \left( Ph_j + \frac{\rho_j}{2} + \frac{\rho_j}{2Lh_j} \right), & j \in [1, n], \end{cases} \quad (14)$$

which are the contributions of the  $j$ -th time-interval to the global error  $E(h, t, \rho)$ . Algorithms 3 and 4 reduce individual components by recursively adjusting the space-time discretization according to the rules

$$\begin{aligned} \psi_h[h, j] &:= \begin{cases} h, & j = 0, \\ (h_1, \dots, h_{j-1}, h_j/2, h_j/2, h_{j+1}, \dots, h_n), & j \in [1, n], \end{cases} \\ \psi_t[t, j] &:= \begin{cases} t, & j = 0, \\ (t_0, \dots, t_{j-1}, t_j - h_j/2, t_j, t_{j+1}, \dots, t_n), & j \in [1, n], \end{cases} \\ \psi_\rho[\rho, j] &:= \begin{cases} (\rho_0/4, \rho_1, \dots, \rho_n), & j = 0, \\ (\rho_0, \dots, \rho_{j-1}, \rho_j/4, \rho_j/4, \rho_{j+1}, \dots, \rho_n), & j \in [1, n]. \end{cases} \end{aligned} \quad (15)$$

When  $j > 0$ , these rules subdivide the  $j$ -th time-interval and adjust the spatial mesh in such a way that the local errors induced by the temporal and spatial discretization are balanced, see Lemma 4.3 below and [10, Remark 3]. When  $j = 0$ , the spatial discretization  $\rho_0$  of the initial set  $X_0$  is refined. Algorithms 3 and 4 differ in the way they choose the interval to be subdivided.

#### 4.1 Error-informed subdivision

Algorithm 3 refines a space-time discretization by subdividing the time-interval whose subdivision leads to the greatest decrease in error (21). This subdivision is carried out recursively according to the rules (15) until the corresponding discrete reachable sets satisfy a given error bound. Algorithm 3 ignores the computational complexity that a subdivision step induces in Algorithm 1.

Algorithm 3 is the closest strategy to classical adaptive quadrature that is feasible in the present context, and should be explored for this reason. Studying Algorithm 3 also allows us to verify that the complexity estimation in Algorithm 4 contributes something that cannot be achieved by working only with the effect of the discretization on the error. In particular, it indicates that the analysis of Algorithm 4, which is the key contribution of this paper, is really worth doing.

---

**Algorithm 3:** Euler scheme with discretization determined by recursively subdividing time-interval for maximal decrease in global error. For the definitions of  $E$  and  $\Delta E$  see (13) and (21).

---

**Input:** Error tolerance  $\varepsilon > 0$

**Output:** Number  $m \in \mathbb{N}$  of iterations carried out,

Number of time-steps  $n_m$ ,

Discretization  $(h^{(m)}, t^{(m)}, \rho^{(m)}) \in \mathbb{R}_{>0}^{n_m} \times \mathbb{R}_{>0}^{n_m+1} \times \mathbb{R}_{>0}^{n_m+1}$ ,

Reachable sets  $R_{h^{(m)}, \rho^{(m)}}^F(k) \subset \rho_k^{(m)} \mathbb{Z}^d$ ,  $k = 0, \dots, n_m$

```

1  $m \leftarrow 0$ ;
2  $n_0 \leftarrow 1$ ;
3  $h^{(0)} \leftarrow (T)$ ;
4  $t^{(0)} \leftarrow (0, T)$ ;
5  $\rho^{(0)} \leftarrow (2LPT^2, 2LPT^2)$ ;
6 while  $E(h^{(m)}, t^{(m)}, \rho^{(m)}) > \varepsilon$  do
7    $k_m \leftarrow \operatorname{argmax}_j (-\Delta E(h^{(m)}, t^{(m)}, \rho^{(m)}; j))$ ;
8   if  $k_m = 0$  then
9      $n_{m+1} \leftarrow n_m$ ;
10  else
11     $n_{m+1} \leftarrow n_m + 1$ ;
12     $h^{(m+1)} \leftarrow \psi_h[h^{(m)}, k_m]$ ;
13     $t^{(m+1)} \leftarrow \psi_t[t^{(m)}, k_m]$ ;
14     $\rho^{(m+1)} \leftarrow \psi_\rho[\rho^{(m)}, k_m]$ ;
15     $m \leftarrow m + 1$ 
16  $(R_{h^{(m)}, \rho^{(m)}}^F, \sim, \sim) \leftarrow [\text{Algorithm 1}](h^{(m)}, t^{(m)}, \rho^{(m)})$ ;
```

---

As a consequence of the subdivision rules (15), the discretizations Algorithm 3 generates have the properties listed in Lemma 4.1. (The same holds for Algorithm 4, which is analyzed in the next section, for the same reasons.) An interpretation of these properties is given in Remark 4.2.

**Lemma 4.1.** *Let  $N \in \mathbb{N}_1$ , and let the sequences  $(h^{(m)})_{m=0}^N$ ,  $(t^{(m)})_{m=0}^N$ ,  $(\rho^{(m)})_{m=0}^N$ ,  $(k_m)_{m=0}^N$ , and  $(n_m)_{m=0}^N$  be generated by Algorithm 3. Then for all  $m \in [0, N]$ , the vectors  $h^{(m)}$ ,  $t^{(m)}$  and  $\rho^{(m)}$  satisfy*

$$(\forall j \in [1, n_m]) (\exists \ell_j^{(m)} \in \mathbb{N}) (h_j^{(m)} = 2^{-\ell_j^{(m)}} T), \quad (16)$$

$$\rho_j^{(m)} = 2LP \left( h_j^{(m)} \right)^2 \quad \forall j \in [1, n_m], \quad (17)$$

$$(\forall j \in [0, n_m]) (\exists i_j^{(m)} \in \mathbb{N}) (t_j^{(m)} = i_j^{(m)} h_j^{(m)}). \quad (18)$$

$$t^{(m)} = \Sigma_+ h^{(m)}, \quad (19)$$

**Remark 4.2.** *Informally speaking, Lemma 4.1 tells us that at any stage of the algorithm, we know that*

- *the  $j$ -th time-interval has the diameter  $2^{-\ell_j} T$  for some  $\ell_j \in \mathbb{N}$ ,*
- *the diameter of a time-interval is coupled with the spatial discretization at its endpoint,*
- *the endpoints of a time-interval are integer multiples of its diameter,*
- *the temporal nodes and the step-sizes match.*

*Proof of Lemma 4.1.* We carry out an induction on  $m$ . All statements are true for  $m = 0$ , when we have  $h^{(0)} = (T) \in \mathbb{R}$ ,  $t^{(0)} = (0, T) \in \mathbb{R}^2$ , and  $\rho^{(0)} = (2LPT^2, 2LPT^2) \in \mathbb{R}^2$ .

Now assume that all statements hold for some  $m \in \mathbb{N}$ . If  $k_m = 0$ , then obviously, all statements hold for  $m + 1$  as well. If  $k_m > 0$ , then the rules (15) and the induction hypothesis imply the representations

$$h_j^{(m+1)} = \begin{cases} h_j^{(m)}, & j < k_m, \\ \frac{h_{k_m}^{(m)}}{2}, & j = k_m, \\ \frac{h_{k_m}^{(m)}}{2}, & j = k_m + 1, \\ h_{j-1}^{(m)}, & j > k_m + 1, \end{cases}$$

$$\rho_j^{(m+1)} = \begin{cases} \rho_j^{(m)} = 2LP(h_j^{(m)})^2 = 2LP(h_j^{(m+1)})^2, & j < k_m, \\ \frac{1}{4}\rho_{k_m}^{(m)} = \frac{1}{2}LP(h_{k_m}^{(m)})^2 = 2LP(h_{k_m}^{(m+1)})^2, & j = k_m, \\ \frac{1}{4}\rho_{k_m}^{(m)} = \frac{1}{2}LP(h_{k_m}^{(m)})^2 = 2LP(h_{k_m+1}^{(m+1)})^2, & j = k_m + 1, \\ \rho_{j-1}^{(m)} = 2LP(h_{j-1}^{(m)})^2 = 2LP(h_j^{(m+1)})^2, & j > k_m + 1, \end{cases}$$

$$t_j^{(m+1)} = \begin{cases} t_j^{(m)} = i_j^{(m)} h_j^{(m)} = i_j^{(m)} h_j^{(m+1)}, & j < k_m, \\ t_{k_m}^{(m)} - \frac{h_{k_m}^{(m)}}{2} = (2i_{k_m}^{(m)} - 1)(\frac{h_{k_m}^{(m)}}{2}) \\ \quad = (2i_{k_m}^{(m)} - 1)h_{k_m}^{(m+1)}, & j = k_m, \\ t_{k_m}^{(m)} = (2i_{k_m}^{(m)})\frac{h_{k_m}^{(m)}}{2} = (2i_{k_m}^{(m)})h_{k_m+1}^{(m+1)}, & j = k_m + 1, \\ t_{j-1}^{(m)} = i_{j-1}^{(m)} h_{j-1}^{(m)} = i_{j-1}^{(m)} h_j^{(m+1)}, & j > k_m + 1, \end{cases}$$

so equations (16), (17), and (18) hold for  $m + 1$ . By checking

$$t_j^{(m+1)} = \begin{cases} t_j^{(m)} = \sum_{s=1}^j h_s^{(m)} = \sum_{s=1}^j h_s^{(m+1)}, & j < k_m, \\ t_{k_m}^{(m)} - \frac{h_{k_m}^{(m)}}{2} = \sum_{s=1}^{k_m} h_s^{(m)} - \frac{h_{k_m}^{(m)}}{2} \\ \quad = \sum_{s=1}^{k_m-1} h_s^{(m+1)} + \frac{h_{k_m}^{(m)}}{2} \\ \quad = \sum_{s=1}^{k_m} h_s^{(m+1)}, & j = k_m, \\ t_{k_m}^{(m)} = \sum_{s=1}^{k_m} h_s^{(m)} \\ \quad = \sum_{s=1}^{k_m-1} h_s^{(m+1)} + \frac{h_{k_m}^{(m)}}{2} + \frac{h_{k_m}^{(m)}}{2} \\ \quad = \sum_{s=1}^{k_m+1} h_s^{(m+1)}, & j = k_m + 1, \\ t_{j-1}^{(m)} = \sum_{s=1}^{j-1} h_s^{(m)} = \sum_{s=1}^j h_s^{(m+1)}, & j > k_m + 1, \end{cases}$$

we can confirm (19) holds for  $m + 1$  as well.  $\square$

The following lemma quantifies how the subdivision rules (15) affect the components  $\mathcal{E}_n^j(h, t, \rho)$ . By Lemma 4.1, condition (20) is satisfied at runtime of Algorithm 3. (Again, the same applies to Algorithm 4 for the same reasons.)

**Lemma 4.3.** *Let  $h \in \mathbb{R}^n$ ,  $t \in \mathbb{R}^{n+1}$  and  $\rho \in \mathbb{R}^{n+1}$  with*

$$t = \Sigma_+ h \quad \text{and} \quad \rho_j = 2LP(h_j)^2 \quad \forall j \in [1, n]. \quad (20)$$

*Then for any  $k \in [0, n]$ , the quantity*

$$\Delta E(h, t, \rho; k) := E(\psi_h[h, k], \psi_t[t, k], \psi_\rho[\rho, k]) - E(h, t, \rho) \quad (21)$$

satisfies

$$\begin{aligned}\Delta E(h, t, \rho; k) &= \begin{cases} -\frac{3e^{LT}}{8}\rho_0, & k = 0, \\ -e^{L(T-t_k)}(e^{Lh_k} - 1) \left( Ph_k + \frac{3LP h_k^2}{4} \right), & k \in [1, n], \end{cases} \\ &\leq \begin{cases} -\frac{1}{2}\mathcal{E}_0(h, t, \rho), & k = 0, \\ -\frac{1}{2}\mathcal{E}_k(h, t, \rho), & k \in [1, n]. \end{cases}\end{aligned}$$

*Proof.* In the following computations, all addends that are not affected by the interval subdivision cancel out. When  $k = 0$ , we observe that

$$\mathcal{E}_j(\psi_h[h, 0], \psi_t[t, 0], \psi_\rho[\rho, 0]) = \mathcal{E}_j(h, t, \rho) \quad \forall j \in [1, k],$$

so we have

$$\begin{aligned}\Delta E(h, t, \rho; 0) &= E(\psi_h[h, 0], \psi_t[t, 0], \psi_\rho[\rho, 0]) - E(h, t, \rho) \\ &= \sum_{j=0}^n \mathcal{E}_j(\psi_h[h, 0], \psi_t[t, 0], \psi_\rho[\rho, 0]) - \sum_{j=0}^n \mathcal{E}_j(h, t, \rho) \\ &= \mathcal{E}_0(\psi_h[h, 0], \psi_t[t, 0], \psi_\rho[\rho, 0]) - \mathcal{E}_0(h, t, \rho) \\ &= e^{LT}\frac{\rho_0}{8} - e^{LT}\frac{\rho_0}{2} = -\frac{3e^{LT}}{8}\rho_0 \leq -\frac{e^{LT}}{4}\rho_0 = -\frac{1}{2}\mathcal{E}_0(h, t, \rho).\end{aligned}$$

When  $k \in [1, n]$ , we observe that

$$\mathcal{E}_j(\psi_h[h, k], \psi_t[t, k], \psi_\rho[\rho, k]) = \begin{cases} \mathcal{E}_j(h, t, \rho), & j \in [0, k-1], \\ \mathcal{E}_{j-1}(h, t, \rho), & j \in [k+2, n+1], \end{cases}$$

so using the abbreviations  $\tilde{h} := \psi_h[h, k]$ ,  $\tilde{t} := \psi_t[t, k]$  and  $\tilde{\rho} := \psi_\rho[\rho, k]$ , we compute

$$\begin{aligned}\Delta E(h, t, \rho; k) &= E(\tilde{h}, \tilde{t}, \tilde{\rho}) - E(h, t, \rho) \\ &= \sum_{j=0}^{n+1} \mathcal{E}_j(\tilde{h}, \tilde{t}, \tilde{\rho}) - \sum_{j=0}^n \mathcal{E}_j(h, t, \rho) = \mathcal{E}_k(\tilde{h}, \tilde{t}, \tilde{\rho}) + \mathcal{E}_{k+1}(\tilde{h}, \tilde{t}, \tilde{\rho}) - \mathcal{E}_k(h, t, \rho) \\ &= e^{L(T-\tilde{t}_k)}(e^{L\tilde{h}_k} - 1) \left( P\tilde{h}_k + \frac{\tilde{\rho}_k}{2} + \frac{\tilde{\rho}_k}{2L\tilde{h}_k} \right) \\ &\quad + e^{L(T-\tilde{t}_{k+1})}(e^{L\tilde{h}_{k+1}} - 1) \left( P\tilde{h}_{k+1} + \frac{\tilde{\rho}_{k+1}}{2} + \frac{\tilde{\rho}_{k+1}}{2L\tilde{h}_{k+1}} \right) \\ &\quad - e^{L(T-t_k)}(e^{Lh_k} - 1) \left( Ph_k + \frac{\rho_k}{2} + \frac{\rho_k}{2Lh_k} \right)\end{aligned}$$

$$\begin{aligned}
&= e^{L(T-t_k+\frac{h_k}{2})}(e^{L\frac{h_k}{2}}-1)\left(\frac{Ph_k}{2}+\frac{\rho_k}{8}+\frac{\rho_k}{4Lh_k}\right) \\
&\quad + e^{L(T-t_k)}(e^{L\frac{h_k}{2}}-1)\left(\frac{Ph_k}{2}+\frac{\rho_k}{8}+\frac{\rho_k}{4Lh_k}\right) \\
&\quad - e^{L(T-t_k)}(e^{Lh_k}-1)\left(Ph_k+\frac{\rho_k}{2}+\frac{\rho_k}{2Lh_k}\right) \\
&= e^{L(T-t_k)}(e^{Lh_k}-1)\left(\left(\frac{Ph_k}{2}+\frac{\rho_k}{8}+\frac{\rho_k}{4Lh_k}\right)-\left(Ph_k+\frac{\rho_k}{2}+\frac{\rho_k}{2Lh_k}\right)\right) \\
&= e^{L(T-t_k)}(e^{Lh_k}-1)\left(-\frac{1}{2}Ph_k-\frac{3}{8}\rho_k-\frac{1}{4}\frac{\rho_k}{Lh_k}\right) \\
&= -e^{L(T-t_k)}(e^{Lh_k}-1)\left(Ph_k+\frac{3}{4}LPh_k^2\right),
\end{aligned}$$

where the final step is due to the second part of statement (20). In particular, we have

$$\begin{aligned}
\Delta E(h, t, \rho; k) &= -e^{L(T-t_k)}(e^{Lh_k}-1)\left(Ph_k+\frac{3}{4}LPh_k^2\right) \\
&\leq -e^{L(T-t_k)}(e^{Lh_k}-1)\left(Ph_k+\frac{1}{2}LPh_k^2\right) = -\frac{1}{2}\mathcal{E}_k(h, t, \rho).
\end{aligned}$$

□

Now we prove that Algorithm 3 converges in finite time.

**Theorem 4.4.** *If Algorithm 3 has not terminated after  $m$  iterations, then*

$$E(h^{(m)}, t^{(m)}, \rho^{(m)}) \leq E(h^{(0)}, t^{(0)}, \rho^{(0)}) \prod_{j=1}^m \left(1 - \frac{1}{2(j+1)}\right). \quad (22)$$

*In particular, for every  $\varepsilon > 0$ , there exists  $m \in \mathbb{N}$  such that Algorithm 3 terminates after  $m$  steps and returns a discretization  $(h^{(m)}, t^{(m)}, \rho^{(m)})$  with*

$$E(h^{(m)}, t^{(m)}, \rho^{(m)}) \leq \varepsilon.$$

*Proof.* We prove statement (22) through induction on  $m$ . When  $m = 0$ , this is trivially satisfied. Now assume that statement (22) holds for some  $m$ . Line 7 of Algorithm 3 implies

$$-\Delta E(h^{(m)}, t^{(m)}, \rho^{(m)}; k_m) \geq -\Delta E(h^{(m)}, t^{(m)}, \rho^{(m)}; j) \quad \forall j \in [0, n_m].$$



By Lemma 4.1, condition (20) in Lemma 4.3 holds. Using Lemma 4.3 and the above inequality, we obtain that

$$\begin{aligned}
E(h^{(m)}, t^{(m)}, \rho^{(m)}) &= \sum_{j=0}^{n_m} \mathcal{E}_j(h^{(m)}, t^{(m)}, \rho^{(m)}) \\
&\leq -2 \sum_{j=0}^{n_m} \Delta E(h^{(m)}, t^{(m)}, \rho^{(m)}; j) \\
&\leq -2(n_m + 1) \Delta E(h^{(m)}, t^{(m)}, \rho^{(m)}; k_m) \\
&\leq -2(m + 2) \Delta E(h^{(m)}, t^{(m)}, \rho^{(m)}; k_m),
\end{aligned}$$

and so, using the induction hypothesis, we have

$$\begin{aligned}
E(h^{(m+1)}, t^{(m+1)}, \rho^{(m+1)}) &= E(h^{(m)}, t^{(m)}, \rho^{(m)}) + \Delta E(h^{(m)}, t^{(m)}, \rho^{(m)}; k_m) \\
&\leq E(h^{(m)}, t^{(m)}, \rho^{(m)}) \left(1 - \frac{1}{2(m+2)}\right) \\
&\leq E(h^{(0)}, t^{(0)}, \rho^{(0)}) \prod_{j=1}^{m+1} \left(1 - \frac{1}{2(j+1)}\right).
\end{aligned}$$

Thus statement (22) holds for  $m + 1$  as well, and hence for all  $m \in \mathbb{N}$ . Since the sequence  $(a_m)_m$  given by

$$a_m := \prod_{j=1}^m \left(1 - \frac{1}{2(j+1)}\right)$$

is strictly positive and monotone decreasing, it is convergent. As the harmonic series diverges, Theorem 28.4 in [21] guarantees that  $\lim_{m \rightarrow \infty} a_m = 0$ . In particular, Algorithm 3 terminates after finitely many steps.  $\square$

Algorithm 3 does not take into account that the subdivision of an interval comes at a cost. This is the motivation for Algorithm 4, which is proposed in the next section.

## 4.2 Utility-informed subdivision

In this section, we develop and analyze Algorithm 4. It recursively refines a space-time discretization by subdividing the time-interval with maximal utility, given by the quotient of the decrease in error bound (13) and the increase in computational cost for executing Algorithm 1 caused by the corresponding subdivision, see line 14 of Algorithm 4.

The increase in computational cost induced by the subdivision of a time-interval can only be estimated, because it depends on the exact shape and location of the discrete reachable sets to be computed. This is the key difference between Algorithm 4 and classical subdivision algorithms like adaptive quadrature, where the cost of a subdivision step is obvious. The analysis of Algorithm 4 is more complicated than that of Algorithm 3, because subdividing an interval changes the estimated cost not only of the subdivided interval, but also of adjacent intervals.

We develop an estimator for the computational cost of Algorithm 1 that uses a current best guess for the sizes and other quantities associated with the desired reachable sets.

**Remark 4.5.** *We estimate the cost of running Algorithm 1 using the following heuristic: Assume that the images  $F(x)$  of  $F$  are  $d_F$ -dimensional, and that the reachable sets  $R^F(t)$  are  $d_R$ -dimensional. Suppose Algorithm 1 has already been run with a relatively coarse discretization*

$$(\tilde{h}, \tilde{t}, \tilde{\rho}) \in \mathbb{R}_{>0}^{\tilde{n}} \times \mathbb{R}^{\tilde{n}+1} \times \mathbb{R}_{>0}^{\tilde{n}+1},$$

and that it has returned the empirical volumes

$$\tilde{R}_k := \#R_{\tilde{h}, \tilde{\rho}}^F(k) \cdot \tilde{\rho}_k^{d_R} \in \mathbb{R}_{>0}, \quad k = 0, \dots, \tilde{n}, \quad (23)$$

of the discrete reachable sets, and the empirical averages

$$\tilde{F}_k := \left( \frac{\tilde{\rho}_{k+1}}{\tilde{h}_{k+1}} \right)^{d_F} \cdot \frac{\sum_{x \in R_{\tilde{h}, \tilde{\rho}}^F(k)} (\# \pi_{\tilde{\rho}_{k+1}}(x + \tilde{h}_{k+1} F(x)))}{\# R_{\tilde{h}, \tilde{\rho}}^F(k)} \in \mathbb{R}_{>0} \quad (24)$$

for  $k = 0, \dots, \tilde{n} - 1$  and  $\tilde{F}_{\tilde{n}} := \tilde{F}_{\tilde{n}-1} \in \mathbb{R}_{>0}$ , which are the volumes of the images of the mapping  $F$  over the individual reachable sets. When we interpolate the data  $(\tilde{t}_k, \tilde{R}_k)_{k=0}^{\tilde{n}}$  and  $(\tilde{t}_k, \tilde{F}_k)_{k=0}^{\tilde{n}}$  with piecewise linear splines

$$v_R : [0, 1] \rightarrow \mathbb{R}_{>0} \quad \text{and} \quad v_F : [0, 1] \rightarrow \mathbb{R}_{>0}$$

and run Algorithm 1 again with a discretization

$$(h, t, \rho) \in \mathbb{R}_{>0}^n \times \mathbb{R}^{n+1} \times \mathbb{R}_{>0}^{n+1}$$

finer than  $(\tilde{h}, \tilde{t}, \tilde{\rho})$ , we expect (by continuity of all constructions involved and because of Theorem 3.3) that the empirical volumes  $R_0, \dots, R_n \in \mathbb{R}_{>0}$  of the

resulting reachable sets and the empirical average volumes  $F_0, \dots, F_n \in \mathbb{R}_{>0}$  of  $F$  over these reachable sets satisfy

$$R_k \approx v_R(t_k), \quad F_k \approx v_F(t_k), \quad k = 0, \dots, n, \quad (25)$$

and that the accuracy of these estimates increases as

$$\max\{\|\tilde{h}\|_\infty, \|\tilde{\rho}\|_\infty, \|h\|_\infty, \|\rho\|_\infty\} \rightarrow 0.$$

Hence the cost Algorithm 1 with discretization  $(h, t, \rho)$  incurs in the time-interval  $[t_\ell, t_{\ell+1}]$  is approximately

$$\mathcal{C}_\ell(h, t, \rho) := \frac{v_R(t_\ell)}{\rho_\ell^{d_R}} \frac{v_F(t_\ell) h_{\ell+1}^{d_F}}{\rho_{\ell+1}^{d_F}} \approx \frac{R_\ell}{\rho_\ell^{d_R}} \frac{F_\ell h_{\ell+1}^{d_F}}{\rho_{\ell+1}^{d_F}}, \quad (26)$$

because  $R_\ell/\rho_\ell^{d_R}$  is the number of grid points in  $R_{h,\rho}^F(\ell)$ , and for every single grid point  $x \in R_{h,\rho}^F(\ell)$ , roughly  $F_\ell h_{\ell+1}^{d_F}/\rho_{\ell+1}^{d_F}$  grid points in the Euler image  $x + h_{\ell+1}F(x)$  have to be computed. All in all, we arrive at the estimator

$$C(h, t, \rho) := \sum_{\ell=0}^{n-1} \mathcal{C}_\ell(h, t, \rho) \quad (27)$$

for the total cost incurred by Algorithm 1 with discretization  $(h, t, \rho)$ . Here we suppress the dependence of  $C(h, t, \rho)$  and  $\mathcal{C}_\ell(h, t, \rho)$  on  $v_R(t_\ell)$  and  $v_F(t_\ell)$  in the notation to maintain the readability of the document.

We are aware that there are situations in which this estimator is not very accurate. However, Theorem 4.10 shows that it is sufficient from a theoretical perspective, and the numerical examples in Section 5 suggest that the performance of Algorithm 4 with the above estimator is very good. For a detailed analysis see Example 5.2, Tables 2 and 3, and Figure 4.

Now we begin to collect evidence for the convergence of Algorithm 4, which we will prove by contradiction. Since Algorithm 4 uses the same subdivision rules (15) as Algorithm 3, Lemmas 4.1 and 4.3 hold when applied to Algorithm 4.

**Lemma 4.6.** *Assume that Algorithm 4 does not terminate, and that it generates the sequences  $(h^{(m)})_{m=0}^\infty$ ,  $(t^{(m)})_{m=0}^\infty$ ,  $(\rho^{(m)})_{m=0}^\infty$ ,  $(k_m)_{m=0}^\infty$ , and  $(n_m)_{m=0}^\infty$ . Then we have*

$$\lim_{m \rightarrow \infty} \Delta E(h^{(m)}, t^{(m)}, \rho^{(m)}; k_m) = 0, \quad (28)$$

as well as

$$\lim_{m \rightarrow \infty} \rho_{k_m}^{(m)} = 0 \quad \text{and} \quad \lim_{\substack{m \rightarrow \infty \\ k_m \neq 0}} h_{k_m}^{(m)} = 0. \quad (29)$$

---

**Algorithm 4:** Iterative refinement procedure based on Euler's scheme with discretization determined by subdividing time-interval with greatest benefit per cost. For the definitions of  $E$ ,  $\Delta E$  and  $\Delta C$  see (13), (21) and (32).

---

**Input:** Recalculation thresholds  $\varepsilon_1 > \varepsilon_2 > \dots > \varepsilon_{\ell_{\max}} > 0$

**Output:** Numbers  $m \in \mathbb{N}$  of iterations carried out,

Number of time-steps  $n_m$ ,

Discretization  $(h^{(m)}, t^{(m)}, \rho^{(m)}) \in \mathbb{R}_{>0}^{n_m} \times \mathbb{R}_{>0}^{n_m+1} \times \mathbb{R}_{>0}^{n_m+1}$ ,

Reachable sets  $R_{h^{(m)}, \rho^{(m)}}^F(k) \subset \rho_k^{(m)} \mathbb{Z}^d$ ,  $k = 0, \dots, n_m$

```

1   $n_0 \leftarrow 1$ ;
2   $h^{(0)} \leftarrow (T)$ ;
3   $t^{(0)} \leftarrow (0, T)$ ;
4   $\rho^{(0)} \leftarrow (2LPT^2, 2LPT^2)$ ;
5   $m \leftarrow 0$ ;
6   $\ell \leftarrow 0$ ;
7  while  $\ell \leq \ell_{\max}$  do
8      if  $m = 0$  or  $E(h^{(m)}, t^{(m)}, \rho^{(m)}) \leq \varepsilon_\ell$  then
9           $(R_{h^{(m)}, \rho^{(m)}}^F, R^{(m)}, F^{(m)}) \leftarrow [\text{Algorithm 1}](h^{(m)}, t^{(m)}, \rho^{(m)})$ ;
10          $v_R^{(m)} \leftarrow [\text{linear spline}](t^{(m)}, R^{(m)})$ ;
11          $v_F^{(m)} \leftarrow [\text{linear spline}](t^{(m)}, F^{(m)})$ ;
12          $\ell \leftarrow \ell + 1$ ;
13     else
14          $k_m \leftarrow \arg \max_j \frac{-\Delta E(h^{(m)}, t^{(m)}, \rho^{(m)}; j)}{\Delta C(h^{(m)}, t^{(m)}, \rho^{(m)}, v_R^{(m)}, v_F^{(m)}; j)}$ ;
15         if  $k_m = 0$  then
16              $n_{m+1} \leftarrow n_m$ ;
17         else
18              $n_{m+1} \leftarrow n_m + 1$ ;
19          $h^{(m+1)} \leftarrow \psi_h[h^{(m)}, k_m]$ ;
20          $t^{(m+1)} \leftarrow \psi_t[t^{(m)}, k_m]$ ;
21          $\rho^{(m+1)} \leftarrow \psi_\rho[\rho^{(m)}, k_m]$ ;
22          $v_R^{(m+1)} \leftarrow v_R^{(m)}$ ;
23          $v_F^{(m+1)} \leftarrow v_F^{(m)}$ ;
24          $m \leftarrow m + 1$ ;

```

---

*Proof.* By Lemma 4.3, we have

$$\Delta E(h^{(m)}, t^{(m)}, \rho^{(m)}; k_m) \leq 0 \quad \forall m \in \mathbb{N},$$

and by construction, we have

$$\begin{aligned} -E(h^{(0)}, t^{(0)}, \rho^{(0)}) &\leq E(h^{(m)}, t^{(m)}, \rho^{(m)}) - E(h^{(0)}, t^{(0)}, \rho^{(0)}) \\ &= \sum_{j=1}^{m-1} \Delta E(h^{(j)}, t^{(j)}, \rho^{(j)}; k_j), \end{aligned}$$

which implies statement (28). Using Lemma 4.3, the identity (14) and the fact that  $e^{Ls} \geq (1 + Ls)$  for all  $s \in \mathbb{R}$ , we conclude that

$$\begin{aligned} \Delta E(h^{(m)}, t^{(m)}, \rho^{(m)}; k_m) &\leq -\frac{1}{2} \mathcal{E}_{k_m}(h^{(m)}, t^{(m)}, \rho^{(m)}) \\ &= -\frac{1}{2} \begin{cases} e^{LT \frac{\rho_{k_m}}{2}}, & k_m = 0, \\ e^{L(T-t_{k_m})} (e^{Lh_{k_m}} - 1) \left( Ph_{k_m} + \frac{\rho_{k_m}}{2} + \frac{\rho_{k_m}}{2Lh_{k_m}} \right), & k_m \in [1, n] \end{cases} \\ &\leq -\frac{1}{2} \begin{cases} e^{LT \frac{\rho_{k_m}}{2}}, & k_m = 0, \\ e^{L(T-t_{k_m})} \frac{\rho_{k_m}}{2}, & k_m \in [1, n] \end{cases} \leq -\frac{1}{4} \rho_{k_m}^{(m)}, \end{aligned}$$

which, together with statement (28), implies the first part of statement (29). Finally, the first part of statement (29), combined with Lemma 4.1 then provides the second part of statement (29).  $\square$

The following technical lemma will be needed in the proof of Proposition 4.8. Lemma 4.7 states that Algorithm 4 relabels, but never discards any previously computed nodes  $t_j^{(m)}$ .

**Lemma 4.7.** *Assume that Algorithm 4 does not terminate, and that it generates the sequences  $(h^{(m)})_{m=0}^\infty$ ,  $(t^{(m)})_{m=0}^\infty$ ,  $(\rho^{(m)})_{m=0}^\infty$ ,  $(k_m)_{m=0}^\infty$ , and  $(n_m)_{m=0}^\infty$ . Then for every  $m_0 \in \mathbb{N}$  and  $j \in [0, n_{m_0}]$ , there exists a monotone increasing sequence  $(j_m)_{m=m_0}^\infty$  with  $j_m \in [0, n_m]$  for all  $m \in [m_0, \infty)$  and*

$$t_j^{(m_0)} = t_{j_m}^{(m)} \quad \forall m \in [m_0, \infty).$$

*Proof.* We prove this lemma by induction on  $m$ . When  $m = m_0$ , we choose the index  $j_{m_0} = j$ . If we have constructed  $(j_\ell)_{\ell=m_0}^m$  for some  $m \in [m_0, \infty)$ , and if  $t_j^{(m_0)} = t_{j_m}^{(m)}$ , then line 20 of Algorithm 4 assigns

$$t_{j_m}^{(m)} = \begin{cases} t_{j_m}^{(m+1)}, & k_m = 0, \\ t_{j_m+1}^{(m+1)}, & k_m \in [1, j_m], \\ t_{j_m}^{(m+1)}, & k_m \in [j_m + 1, n_m], \end{cases}$$

so the index

$$j_{m+1} := \begin{cases} j_m, & k_m = 0, \\ j_m + 1, & k_m \in [1, j_m], \\ j_m, & k_m \in [j_m + 1, n_m] \end{cases}$$

satisfies  $t_j^{(m_0)} = t_{j_{m+1}}^{(m+1)}$ .  $\square$

Next, we show that if the maximal step-size  $\|h^{(m)}\|_\infty$  in Algorithm 4 does not converge to zero, then there exists a subinterval  $[\tau_-, \tau_+] \subset [0, T]$  that is never subdivided.

**Proposition 4.8.** *Assume that Algorithm 4 does not terminate, and that it generates the sequences  $(h^{(m)})_{m=0}^\infty$ ,  $(t^{(m)})_{m=0}^\infty$ ,  $(\rho^{(m)})_{m=0}^\infty$ ,  $(k_m)_{m=0}^\infty$ , and  $(n_m)_{m=0}^\infty$ . If we have*

$$\lim_{m \rightarrow \infty} \|h^{(m)}\|_\infty \neq 0, \quad (30)$$

*then there exist  $\tau_-, \tau_+ \in [0, T]$  and  $m_0 \in \mathbb{N}$  such that  $\tau_- < \tau_+$  and, for all  $m \geq m_0$ , there exists  $j_m \in [1, n_m]$  with*

$$\tau_- = t_{j_m-1}^{(m)} \text{ and } \tau_+ = t_{j_m}^{(m)}.$$

*Proof.* Since  $n_m < \infty$ , by statement (16) in Lemma 4.1, there exist  $\ell_m \in \mathbb{N}$  such that

$$\|h^{(m)}\|_\infty = 2^{-\ell_m} T \quad \forall m \in \mathbb{N},$$

and by construction of  $h^{(m)}$ , the sequence  $(\ell_m)_m$  is monotone increasing. By assumption (30), there exists  $m_0 \in \mathbb{N}$  such that

$$\ell_m = \ell_{m_0} \quad \forall m \in [m_0, \infty),$$

and hence for every  $m \in [m_0, \infty)$ , there exists an index  $j_m \in [1, n_m]$  such that  $h_{j_m}^{(m)} = 2^{-\ell_{m_0}} T$ . By Lemma 4.1, there exist integers  $i_m \in [1, 2^{\ell_{m_0}}]$  with

$$t_{j_m}^{(m)} = i_m h_{j_m}^{(m)} = 2^{-\ell_{m_0}} T i_m \quad \forall m \in [m_0, \infty).$$

Since  $[1, 2^{\ell_{m_0}}]$  is finite, there exist  $i^* \in [1, 2^{\ell_{m_0}}]$  and a subsequence  $\mathbb{N}' \subset \mathbb{N}$  such that

$$i_m = i^* \quad \forall m \in \mathbb{N}'.$$

We define

$$\tau_- := 2^{-\ell_{m_0}} T (i^* - 1) \quad \text{and} \quad \tau_+ := 2^{-\ell_{m_0}} T i^*.$$

It follows that

$$\tau_- = t_{j_m-1}^{(m)} \quad \text{and} \quad \tau_+ = t_{j_m}^{(m)} \quad \forall m \in \mathbb{N}' \cap [m_0, \infty). \quad (31)$$

Let  $m'_0 := \min(\mathbb{N}' \cap [m_0, \infty))$ . By Lemma 4.7, there exist sequences  $(j_m^-)_{m=m'_0}^\infty$  and  $(j_m^+)_{m=m'_0}^\infty$  with

$$\tau_- = t_{j_m^-}^{(m)} \quad \text{and} \quad \tau_+ = t_{j_m^+}^{(m)} \quad \forall m \in [m'_0, \infty).$$

Now we show that

$$j_m^- + 1 = j_m^+ \quad \forall m \in [m'_0, \infty),$$

which completes the proof. Otherwise, there exist integers  $\hat{m} \in [m'_0, \infty)$  and  $\hat{j}_{\hat{m}} \in (j_{\hat{m}}^-, j_{\hat{m}}^+)$  with

$$\tau_- = t_{j_{\hat{m}}^-}^{(\hat{m})} < t_{\hat{j}_{\hat{m}}}^{(\hat{m})} < t_{j_{\hat{m}}^+}^{(\hat{m})} = \tau_+.$$

But then, Lemma 4.7 yields that for

$$m''_0 := \min(\mathbb{N}' \cap [\hat{m}, \infty)),$$

there exists  $\hat{j}_{m''_0} \in [1, n_{m''_0}]$  with  $t_{\hat{j}_{m''_0}}^{(m''_0)} = t_{\hat{j}_{\hat{m}}}^{(\hat{m})}$ . It follows that

$$\tau_- = t_{j_{m''_0}^-}^{(m''_0)} < t_{\hat{j}_{m''_0}}^{(m''_0)} < t_{j_{m''_0}^+}^{(m''_0)} = \tau_+,$$

which forces  $j_{m''_0}^- + 1 < j_{m''_0}^+$  and hence contradicts statement (31).  $\square$

Now we investigate the behavior of the estimator  $C$  from statement (27) when an interval is subdivided according to rule (15). Note that the splines  $v_R$  and  $v_F$  from Remark 4.5 have all properties required by Lemma 4.9.

**Lemma 4.9.** *Consider functions  $v_R, v_F : [0, T] \rightarrow \mathbb{R}_+$ , and a discretization  $(h, t, \rho) \in \mathbb{R}_{>0}^n \times \mathbb{R}^{n+1} \times \mathbb{R}_{>0}^{n+1}$  satisfying  $T = \Sigma_+ h$  and equation (17). Then for any  $k \in [0, n]$ , the quantity*

$$\Delta C(h, t, \rho; k) := C(\psi_h[h, k], \psi_t[t, k], \psi_\rho[\rho, k]) - C(h, t, \rho) \quad (32)$$

with  $\psi_h$ ,  $\psi_t$  and  $\psi_\rho$  as defined in equation (15), with  $C$  as defined in statement (27), and with

$$v(t) := v_R(t) v_F(t), \quad \forall t \in [0, T]$$

satisfies

$$\Delta C(h, t, \rho; k) = \begin{cases} v(0) \left( \frac{4^{d_R-1}}{\rho_0^{d_R}} \right) \left( \frac{h_1}{\rho_1} \right)^{d_F}, & k = 0, \\ v\left(T - \frac{h_n}{2}\right) \left( \frac{2h_k}{\rho_k} \right)^{d_F} \left( \frac{4}{\rho_k} \right)^{d_R} \\ \quad + v(t_{n-1}) \left( \frac{2^{d_F-1}}{\rho_{k-1}^{d_R}} \right) \left( \frac{h_k}{\rho_k} \right)^{d_F}, & k = n, \\ v\left(t_k - \frac{h_k}{2}\right) \left( \frac{2h_k}{\rho_k} \right)^{d_F} \left( \frac{4}{\rho_k} \right)^{d_R} \\ \quad + v(t_k) \left( \frac{4^{d_R-1}}{\rho_k^{d_R}} \right) \left( \frac{h_{k+1}}{\rho_{k+1}} \right)^{d_F} \\ \quad + v(t_{k-1}) \left( \frac{2^{d_F-1}}{\rho_{k-1}^{d_R}} \right) \left( \frac{h_k}{\rho_k} \right)^{d_F}, & \text{otherwise.} \end{cases} \quad (33)$$

Denoting

$$V_L := \inf_{t \in [0, T]} v(t) \quad \text{and} \quad V_U := \sup_{t \in [0, T]} v(t),$$

we find the inclusion

$$\Delta C(h, t, \rho; k) \in [V_L, V_U] \begin{cases} \left( \frac{4^{d_R-1}}{\rho_0^{d_R}} \right) \left( \frac{h_1}{\rho_1} \right)^{d_F}, & k = 0, \\ \left( \frac{2h_k}{\rho_k} \right)^{d_F} \left( \frac{4}{\rho_k} \right)^{d_R} \\ \quad + \left( \frac{2^{d_F-1}}{\rho_{k-1}^{d_R}} \right) \left( \frac{h_k}{\rho_k} \right)^{d_F}, & k = n, \\ \left( \frac{2h_k}{\rho_k} \right)^{d_F} \left( \frac{4}{\rho_k} \right)^{d_R} \\ \quad + \left( \frac{4^{d_R-1}}{\rho_k^{d_R}} \right) \left( \frac{h_{k+1}}{\rho_{k+1}} \right)^{d_F} \\ \quad + \left( \frac{2^{d_F-1}}{\rho_{k-1}^{d_R}} \right) \left( \frac{h_k}{\rho_k} \right)^{d_F}, & \text{otherwise.} \end{cases} \quad (34)$$

In particular, we have

$$\Delta C(h, t, \rho; k) \geq \frac{V_L}{(2LPT^{3/2})^{2d}} \quad \forall k \in [0, n]. \quad (35)$$

*Proof.* We only display the proof of equation (33) and inclusion (34) for the case  $k \in [1, n-1]$ , because the cases  $k = 0$  and  $k = n$  are similar. By definition of  $\psi_h$ ,  $\psi_t$ ,  $\psi_\rho$  and  $\mathcal{C}_j$ , we have

$$\mathcal{C}_j(\psi_h[h, k], \psi_t[t, k], \psi_\rho[\rho, k]) = \begin{cases} \mathcal{C}_j(h, t, \rho), & j \in [0, k-2], \\ \mathcal{C}_{j-1}(h, t, \rho), & j \in [k+2, n+1]. \end{cases} \quad (36)$$



In the following computation, we use the definition (27) of the cost estimator  $C$ , statement (36), which allows us to cancel all but five addends, the definition (26) of  $\mathcal{C}_j$ , and the definition (15) of  $\psi_h$ ,  $\psi_t$  and  $\psi_\rho$ . We obtain

$$\begin{aligned}
\Delta C(h, t, \rho; k) &= C(\psi_h[h, k], \psi_t[t, k], \psi_\rho[\rho, k]) - C(h, t, \rho) \\
&= \sum_{j=0}^n \mathcal{C}_j(\psi_h[h, k], \psi_t[t, k], \psi_\rho[\rho, k]) - \sum_{j=0}^{n-1} \mathcal{C}_j(h, t, \rho) \\
&= \mathcal{C}_{k-1}(\psi_h[h, k], \psi_t[t, k], \psi_\rho[\rho, k]) + \mathcal{C}_k(\psi_h[h, k], \psi_t[t, k], \psi_\rho[\rho, k]) \\
&\quad + \mathcal{C}_{k+1}(\psi_h[h, k], \psi_t[t, k], \psi_\rho[\rho, k]) - \mathcal{C}_{k-1}(h, t, \rho) - \mathcal{C}_k(h, t, \rho) \\
&= \frac{\mathbf{v}_R((\psi_t[t, k])_{k-1})}{(\psi_\rho[\rho, k])_{k-1}^{d_R}} \frac{\mathbf{v}_F((\psi_t[t, k])_{k-1})}{(\psi_\rho[\rho, k])_k^{d_F}} (\psi_h[h, k])_k^{d_F} \\
&\quad + \frac{\mathbf{v}_R((\psi_t[t, k])_k)}{(\psi_\rho[\rho, k])_k^{d_R}} \frac{\mathbf{v}_F((\psi_t[t, k])_k)}{(\psi_\rho[\rho, k])_{k+1}^{d_F}} (\psi_h[h, k])_{k+1}^{d_F} \\
&\quad + \frac{\mathbf{v}_R((\psi_t[t, k])_{k+1})}{(\psi_\rho[\rho, k])_{k+1}^{d_R}} \frac{\mathbf{v}_F((\psi_t[t, k])_{k+1})}{(\psi_\rho[\rho, k])_{k+2}^{d_F}} (\psi_h[h, k])_{k+2}^{d_F} \\
&\quad - \frac{\mathbf{v}_R(t_{k-1})}{\rho_{k-1}^{d_R}} \frac{\mathbf{v}_F(t_{k-1})}{\rho_k^{d_F}} h_k^{d_F} - \frac{\mathbf{v}_R(t_k)}{\rho_k^{d_R}} \frac{\mathbf{v}_F(t_k)}{\rho_{k+1}^{d_F}} h_{k+1}^{d_F} \\
&= \frac{\mathbf{v}_R(t_{k-1})}{\rho_{k-1}^{d_R}} \frac{\mathbf{v}_F(t_{k-1})}{(\frac{\rho_k}{4})^{d_F}} (\frac{h_k}{2})^{d_F} + \frac{\mathbf{v}_R(t_k - \frac{h_k}{2})}{(\frac{\rho_k}{4})^{d_R}} \frac{\mathbf{v}_F(t_k - \frac{h_k}{2})}{(\frac{\rho_k}{4})^{d_F}} (\frac{h_k}{2})^{d_F} \\
&\quad + \frac{\mathbf{v}_R(t_k)}{(\frac{\rho_k}{4})^{d_R}} \frac{\mathbf{v}_F(t_k)}{\rho_{k+1}^{d_F}} h_{k+1}^{d_F} - \frac{\mathbf{v}_R(t_{k-1})}{\rho_{k-1}^{d_R}} \frac{\mathbf{v}_F(t_{k-1})}{\rho_k^{d_F}} h_k^{d_F} \\
&\quad - \frac{\mathbf{v}_R(t_k)}{\rho_k^{d_R}} \frac{\mathbf{v}_F(t_k)}{\rho_{k+1}^{d_F}} h_{k+1}^{d_F} \\
&= \mathbf{v}(t_{k-1}) \left( \frac{(\frac{h_k}{2})^{d_F}}{\rho_{k-1}^{d_R} (\frac{\rho_k}{4})^{d_F}} - \frac{h_k^{d_F}}{\rho_{k-1}^{d_R} \rho_k^{d_F}} \right) + \mathbf{v}(t_k - \frac{h_k}{2}) \frac{(\frac{h_k}{2})^{d_F}}{(\frac{\rho_k}{4})^{d_F} (\frac{\rho_k}{4})^{d_R}} \\
&\quad + \mathbf{v}(t_k) \left( \frac{h_{k+1}^{d_F}}{(\frac{\rho_k}{4})^{d_R} \rho_{k+1}^{d_F}} - \frac{h_{k+1}^{d_F}}{\rho_k^{d_R} \rho_{k+1}^{d_F}} \right) \\
&= \mathbf{v}(t_{k-1}) \left( \frac{(2^{d_F-1}) h_k^{d_F}}{\rho_{k-1}^{d_R} \rho_k^{d_F}} \right) + \mathbf{v}(t_k) \left( \frac{(4^{d_R-1}) h_{k+1}^{d_F}}{\rho_k^{d_R} \rho_{k+1}^{d_F}} \right) \\
&\quad + \mathbf{v}(t_k - \frac{h_k}{2}) \left( 2^{d_F+2d_R} \frac{h_k^{d_F}}{\rho_k^{d_F} \rho_k^{d_R}} \right)
\end{aligned}$$

$$\in [V_L, V_U] \left( \frac{(2^{d_F}-1)h_k^{d_F}}{\rho_{k-1}^{d_R}\rho_k^{d_F}} + \frac{(4^{d_R}-1)h_{k+1}^{d_F}}{\rho_k^{d_R}\rho_{k+1}^{d_F}} + 2^{d_F+2d_R} \frac{h_k^{d_F}}{\rho_k^{d_F}\rho_k^{d_R}} \right).$$

The final step of the above computation is justified because all factors are positive. Statement (35) follows from equations (17) and (34), as well as the fact that  $h_j \leq T$  for all  $j \in [1, n]$ .  $\square$

Finally, we show that Algorithm 4 terminates in finite time.

**Theorem 4.10.** *For any  $\varepsilon_1 > \varepsilon_2 > \dots > \varepsilon_{\ell_{\max}} > 0$ , Algorithm 4 returns a discretization  $(h^{(m)}, t^{(m)}, \rho^{(m)})$  with*

$$E(h^{(m)}, t^{(m)}, \rho^{(m)}) \leq \varepsilon_{\ell_{\max}}$$

*after a finite number  $m \in \mathbb{N}$  of iterations.*

*Proof.* We will prove this theorem by contradiction. Assume throughout that Algorithm 4 does not terminate, and that it generates the sequences  $(h^{(m)})_{m=0}^\infty$ ,  $(t^{(m)})_{m=0}^\infty$ ,  $(\rho^{(m)})_{m=0}^\infty$ ,  $(k_m)_{m=0}^\infty$ , and  $(n_m)_{m=0}^\infty$ . Since  $\ell_{\max} < \infty$ , there exists  $\hat{m} \in \mathbb{N}$  such that

$$v_R^{(m)} = v_R^{(\hat{m})} \quad \text{and} \quad v_F^{(m)} = v_F^{(\hat{m})} \quad \forall m \in [\hat{m}, \infty). \quad (37)$$

Since  $X_0 \neq \emptyset$ , we have  $R_{h^{(\hat{m})}, \rho^{(\hat{m})}}^F(k) \neq \emptyset$  for all  $k \in [0, n_{\hat{m}}]$  by construction of the discrete reachable sets. Hence  $R^{(\hat{m})}, F^{(\hat{m})} \in \mathbb{R}_{>0}^{n_{\hat{m}}}$ , see Algorithm 1 and equations (23) and (24), which implies that the product

$$v^{(\hat{m})} := v_R^{(\hat{m})} v_F^{(\hat{m})}$$

of the linear splines  $v_R^{(\hat{m})}$  and  $v_F^{(\hat{m})}$  satisfies

$$0 < V_L := \min_{t \in [0, T]} v^{(\hat{m})}(t) \leq \max_{t \in [0, T]} v^{(\hat{m})}(t) =: V_U < \infty.$$

The remainder of the proof is split into three major steps.

**Step 1:** We show that

$$\lim_{m \rightarrow \infty} \|h^{(m)}\|_\infty = 0 \quad (38)$$

in a proof by contradiction. This step itself is split into three parts.

**Step 1a:** The cost  $\Delta C(h^{(m)}, t^{(m)}, \rho^{(m)}; k_m)$  of subdividing the interval  $[t_{k_m-1}, t_{k_m}]$  increases with  $m$  at a slower rate than the theoretical cost of subdividing the fixed interval  $[\tau_-, \tau_+]$  defined below.

If statement (38) is false, then by Proposition 4.8, there exist points  $\tau_-, \tau_+ \in [0, T]$  and  $m_0 \in [\hat{m}, \infty)$  such that

$$(\forall m \in [m_0, \infty))(\exists i_m \in [1, n_m])(\tau_- = t_{i_m-1}^{(m)} \text{ and } \tau_+ = t_{i_m}^{(m)}). \quad (39)$$

By Lemma 4.1, we have

$$h_{i_m}^{(m)} = t_{i_m}^{(m)} - t_{i_m-1}^{(m)} = \tau_+ - \tau_- = t_{i_{m_0}}^{(m_0)} - t_{i_{m_0}-1}^{(m_0)} = h_{i_{m_0}}^{(m_0)}, \quad (40)$$

$$\rho_{i_m}^{(m)} = 2LP \left( h_{i_m}^{(m)} \right)^2 = 2LP \left( h_{i_{m_0}}^{(m_0)} \right)^2 = \rho_{i_{m_0}}^{(m_0)} \quad (41)$$

for all  $m \in [m_0, \infty)$ . In particular, we have

$$k_m \neq i_m \quad \forall m \in [m_0, \infty),$$

and by line 14 of Algorithm 4, we have

$$\frac{-\Delta E(h^{(m)}, t^{(m)}, \rho^{(m)}; i_m)}{\Delta C(h^{(m)}, t^{(m)}, \rho^{(m)}; i_m)} \leq \frac{-\Delta E(h^{(m)}, t^{(m)}, \rho^{(m)}; k_m)}{\Delta C(h^{(m)}, t^{(m)}, \rho^{(m)}; k_m)} \quad \forall m \in [m_0, \infty).$$

Recall that the quantities  $\Delta C(h^{(m)}, t^{(m)}, \rho^{(m)}; j)$  depend on  $v_R^{(m)}$  and  $v_F^{(m)}$ , see equations (26), (27) and (32), which are identical with  $v_R^{(\hat{m})}$  and  $v_F^{(\hat{m})}$  for all  $m \in [\hat{m}, \infty)$ , see equation (37). After rearranging the above inequality, we use statements (39), (40) and (41) together with Lemma 4.3, and then Lemma 4.6 to conclude that

$$\begin{aligned} \frac{\Delta C(h^{(m)}, t^{(m)}, \rho^{(m)}; k_m)}{\Delta C(h^{(m)}, t^{(m)}, \rho^{(m)}; i_m)} &\leq \frac{-\Delta E(h^{(m)}, t^{(m)}, \rho^{(m)}; k_m)}{-\Delta E(h^{(m)}, t^{(m)}, \rho^{(m)}; i_m)} \\ &= \frac{\Delta E(h^{(m)}, t^{(m)}, \rho^{(m)}; k_m)}{\Delta E(h^{(m_0)}, t^{(m_0)}, \rho^{(m_0)}; i_{m_0})} \rightarrow 0 \text{ as } m \rightarrow \infty. \end{aligned} \quad (42)$$

**Step 1b:** We identify a subsequence  $\mathbb{N}'' \subset \mathbb{N}$  that satisfies both  $k_m \neq 0$  and  $h_{k_m}^{(m)} = \min_{j \in [1, n_m]} h_j^{(m)}$  for all  $m \in \mathbb{N}''$ .

First, we claim that the set

$$\mathbb{N}' := \{m \geq m_0 : k_m \neq 0\}$$

is infinite. Otherwise, we set

$$\tilde{m} := \max(\mathbb{N}' \cup \{m_0\}) + 1$$

and observe that

$$k_m = 0 \quad \forall m \in [\tilde{m}, \infty). \quad (43)$$

This means that, for all  $m \in [\tilde{m}, \infty)$ , equations (15), (33) and (37) imply

$$\begin{aligned} \Delta C(h^{(m+1)}, t^{(m+1)}, \rho^{(m+1)}; k_{m+1}) &= v^{(\hat{m})}(0) \frac{4^{d_R}-1}{(\rho_0^{(m+1)})^{d_R}} \left( \frac{h_1^{(m+1)}}{\rho_1^{(m+1)}} \right)^{d_F} \\ &= 4^{d_R} v^{(\hat{m})}(0) \frac{4^{d_R}-1}{(\rho_0^{(m)})^{d_R}} \left( \frac{h_1^{(m)}}{\rho_1^{(m)}} \right)^{d_F} = 4^{d_R} \Delta C(h^{(m)}, t^{(m)}, \rho^{(m)}; 0). \end{aligned} \quad (44)$$

At the same time, we have  $i_{m+1} = i_m$  for all  $m \in [\tilde{m}, \infty)$ , and a computation that is similar to the one above (but considers the three different cases  $i_m = 1 = n_m$ ,  $i_m = 1 < n_m$  and  $1 < i_m$ ) yields

$$\Delta C(h^{(m+1)}, t^{(m+1)}, \rho^{(m+1)}; i_{m+1}) \leq 4^{d_R} \Delta C(h^{(m)}, t^{(m)}, \rho^{(m)}; i_m) \quad \forall m \in [\tilde{m}, \infty).$$

These two inequalities imply that

$$\frac{\Delta C(h^{(m+1)}, t^{(m+1)}, \rho^{(m+1)}; k_{m+1})}{\Delta C(h^{(m+1)}, t^{(m+1)}, \rho^{(m+1)}; i_{m+1})} \geq \frac{\Delta C(h^{(m)}, t^{(m)}, \rho^{(m)}; k_m)}{\Delta C(h^{(m)}, t^{(m)}, \rho^{(m)}; i_m)} \quad \forall m \in [\tilde{m}, \infty),$$

and hence, by recursion, that

$$\frac{\Delta C(h^{(m)}, t^{(m)}, \rho^{(m)}; k_m)}{\Delta C(h^{(m)}, t^{(m)}, \rho^{(m)}; i_m)} \geq \frac{\Delta C(h^{(\tilde{m})}, t^{(\tilde{m})}, \rho^{(\tilde{m})}; k_{\tilde{m}})}{\Delta C(h^{(\tilde{m})}, t^{(\tilde{m})}, \rho^{(\tilde{m})}; i_{\tilde{m}})} > 0, \quad \forall m \in [\tilde{m}, \infty),$$

contradicting equation (42). This means that  $\mathbb{N}'$  must be infinite.

Now we claim that the set

$$\mathbb{N}'' := \{m \in \mathbb{N}' : h_{k_m}^{(m)} = \min_{j \in [1, n_m]} h_j^{(m)}\}.$$

is infinite. Otherwise, we take

$$\tilde{m} := \max(\mathbb{N}'' \cup \min(\mathbb{N}')) + 1$$

and find that

$$h_{k_m}^{(m)} > \min_{j \in [1, n_m]} h_j^{(m)} \quad \forall m \in [\tilde{m}, \infty) \cap \mathbb{N}'. \quad (45)$$

We assert by induction that this implies

$$\min_{j \in [1, n_m]} h_j^{(m)} = \min_{j \in [1, n_{\tilde{m}}]} h_j^{(\tilde{m})} \quad \forall m \in [\tilde{m}, \infty). \quad (46)$$

The statement is clearly true for  $m = \tilde{m}$ . Now assume that it holds for some  $m \in [\tilde{m}, \infty)$ . If  $m \in \mathbb{N}'$ , then it follows from statement (45) and statement (16) from Lemma 4.1 that

$$h_{k_m}^{(m)} \geq 2 \min_{j \in [1, n_m]} h_j^{(m)}.$$

In view of the subdivision rules (15), this implies statement (46) with  $m + 1$ . If  $m \notin \mathbb{N}'$ , then  $k_m = 0$ , and the rules (15) imply statement (46) with  $m + 1$  directly. All in all, statement (46) is verified.

However, statement (46) contradicts statement (29) of Lemma 4.6. Hence the set  $\mathbb{N}''$  is indeed infinite.

**Step 1c:** The results of steps 1a and 1b lead to a contradiction.

For every  $m \in \mathbb{N}''$ , we have  $k_m \neq 0$ , and hence inclusion (34) provides

$$\begin{aligned} \Delta C(h^{(m)}, t^{(m)}, \rho^{(m)}; k_m) &\geq V_L \left( \frac{2h_{k_m}^{(m)}}{\rho_{k_m}^{(m)}} \right)^{d_F} \left( \frac{4}{\rho_{k_m}^{(m)}} \right)^{d_R} \\ &= \frac{2^{d_R} V_L}{(LP)^{d_F + d_R}} \frac{1}{(h_{k_m}^{(m)})^{d_F + 2d_R}}. \end{aligned} \quad (47)$$

Similarly, since  $i_m \neq 0$  and  $h_{i_m}^{(m)} = \min_{j \in [1, n_m]} h_j^{(m)}$  for all  $m \in \mathbb{N}''$ , equation (34) and Lemma 4.1 imply for all  $m \in \mathbb{N}''$  the inequality

$$\begin{aligned} &\Delta C(h^{(m)}, t^{(m)}, \rho^{(m)}; i_m) \\ &\leq V_U \left\{ \begin{aligned} &\left( \frac{2h_{i_m}^{(m)}}{\rho_{i_m}^{(m)}} \right)^{d_F} \left( \frac{4}{\rho_{i_m}^{(m)}} \right)^{d_R} \\ &\quad + \left( \frac{2^{d_F} - 1}{(2LP)^{d_R} (h_{i_m-1}^{(m)})^{2d_R}} \right) \left( \frac{h_{i_m}^{(m)}}{\rho_{i_m}^{(m)}} \right)^{d_F}, \quad i_m = n, \\ &\left( \frac{2h_{i_m}^{(m)}}{\rho_{i_m}^{(m)}} \right)^{d_F} \left( \frac{4}{\rho_{i_m}^{(m)}} \right)^{d_R} \\ &\quad + \left( \frac{4^{d_R} - 1}{(\rho_{i_m}^{(m)})^{d_R}} \right) \left( \frac{1}{2LP h_{i_m+1}^{(m)}} \right)^{d_F} \\ &\quad + \left( \frac{2^{d_F} - 1}{(2LP)^{d_R} (h_{i_m-1}^{(m)})^{2d_R}} \right) \left( \frac{h_{i_m}^{(m)}}{\rho_{i_m}^{(m)}} \right)^{d_F}, \quad \text{otherwise,} \end{aligned} \right. \end{aligned}$$

and hence that

$$\begin{aligned}
& \Delta C(h^{(m)}, t^{(m)}, \rho^{(m)}; i_m) \\
& \leq V_U \left( \frac{2h_{i_m}^{(m)}}{\rho_{i_m}^{(m)}} \right)^{d_F} \left( \frac{4}{\rho_{i_m}^{(m)}} \right)^{d_R} + V_U \left( \frac{4^{d_R}-1}{(\rho_{i_m}^{(m)})^{d_R}} \right) \left( \frac{1}{2LP h_{k_m}^{(m)}} \right)^{d_F} \\
& \quad + V_U \left( \frac{2^{d_F}-1}{(2LP)^{d_R} (h_{k_m}^{(m)})^{2d_R}} \right) \left( \frac{h_{i_m}^{(m)}}{\rho_{i_m}^{(m)}} \right)^{d_F}.
\end{aligned} \tag{48}$$

Using inequality (48), as well as equations (40) and (41), and noting that  $h_{k_m}^{(m)} \leq T$  for all  $m \in \mathbb{N}$ , we obtain for every  $m \in \mathbb{N}''$  that

$$\begin{aligned}
& \Delta C(h^{(m)}, t^{(m)}, \rho^{(m)}; i_m) \left( h_{k_m}^{(m)} \right)^{d_F+2d_R} \\
& \leq \left( \frac{2h_{i_m}^{(m)}}{\rho_{i_m}^{(m)}} \right)^{d_F} \left( \frac{4}{\rho_{i_m}^{(m)}} \right)^{d_R} \left( h_{k_m}^{(m)} \right)^{d_F+2d_R} \\
& \quad + \left( \frac{4^{d_R}-1}{(\rho_{i_m}^{(m)})^{d_R}} \right) \left( \frac{1}{2LP} \right)^{d_F} \left( h_{k_m}^{(m)} \right)^{2d_R} \\
& \quad + \left( \frac{2^{d_F}-1}{(2LP)^{d_R}} \right) \left( \frac{h_{i_m}^{(m)}}{\rho_{i_m}^{(m)}} \right)^{d_F} \left( h_{k_m}^{(m)} \right)^{d_F} \\
& \leq \left( \frac{2h_{i_{m_0}}^{(m_0)}}{\rho_{i_{m_0}}^{(m_0)}} \right)^{d_F} \left( \frac{4}{\rho_{i_{m_0}}^{(m_0)}} \right)^{d_R} T^{d_F+2d_R} + \left( \frac{4^{d_R}-1}{(\rho_{i_{m_0}}^{(m_0)})^{d_R}} \right) \left( \frac{1}{2LP} \right)^{d_F} T^{2d_R} \\
& \quad + \left( \frac{2^{d_F}-1}{(2LP)^{d_R}} \right) \left( \frac{h_{i_{m_0}}^{(m_0)}}{\rho_{i_{m_0}}^{(m_0)}} \right)^{d_F} T^{d_F},
\end{aligned} \tag{49}$$

which is constant.

Combining inequalities (49) and (47), we find that, for all  $m \in \mathbb{N}''$ ,

$$\frac{\Delta C(h^{(m)}, t^{(m)}, \rho^{(m)}; k_m)}{\Delta C(h^{(m)}, t^{(m)}, \rho^{(m)}; i_m)} \geq \frac{\frac{2^{d_R} V_L}{V_U (LP)^{d_F+d_R}}}{\Delta C(h^{(m)}, t^{(m)}, \rho^{(m)}; i_m) \left( h_{k_m}^{(m)} \right)^{d_F+2d_R}} > 0.$$

This contradicts equation (42).

All in all, we have proved in an indirect argument that statement (38), the goal of Step 1, holds.

**Step 2:** We show that

$$\lim_{m \rightarrow \infty} \rho_0^{(m)} = 0 \tag{50}$$

in a proof by contradiction.

If equation (50) is false, then the subdivision rules (15) imply that there exists  $\hat{m}_0 \in \mathbb{N}$  such that

$$k_m \neq 0 \quad \forall m \in [\hat{m}_0, \infty).$$

We can then derive a contradiction in the same way as in step 1, with the argument

$$\begin{aligned} \frac{\Delta C(h^{(m)}, t^{(m)}, \rho^{(m)}; k_m)}{\Delta C(h^{(m)}, t^{(m)}, \rho^{(m)}; 0)} &\leq \frac{-\Delta E(h^{(m)}, t^{(m)}, \rho^{(m)}; k_m)}{-\Delta E(h^{(m)}, t^{(m)}, \rho^{(m)}; 0)} \\ &= \frac{\Delta E(h^{(m)}, t^{(m)}, \rho^{(m)}; k_m)}{\Delta E(h^{(\hat{m}_0)}, t^{(\hat{m}_0)}, \rho^{(\hat{m}_0)}; 0)} \rightarrow 0 \text{ as } m \rightarrow \infty \end{aligned}$$

replacing statement (42) in step 1a, the index  $\hat{m}_0$  replacing  $m_0$  in step 1c, and the inequality

$$\Delta C(h^{(m)}, t^{(m)}, \rho^{(m)}; 0) \leq V_U \frac{4^{d_R} - 1}{\left(\rho_0^{(m)}\right)^{d_R}} \left(\frac{1}{2LP h_{k_m}^{(m)}}\right)^{d_F} \quad \forall m \in \mathbb{N}''$$

replacing equation (48) in step 1c.

**Step 3:** Equations (38) and (50) lead to a contradiction.

Since Algorithm 4 does not terminate by assumption, we have

$$E(h^{(m)}, t^{(m)}, \rho^{(m)}) > \varepsilon_{\ell_{max}} > 0 \quad \forall m \in \mathbb{N}. \quad (51)$$

The total error satisfies

$$\begin{aligned} E(h^{(m)}, t^{(m)}, \rho^{(m)}) &= \frac{\rho_0^{(m)}}{2} e^L + P \sum_{j=1}^{n_m} e^{L(1-t_j^{(m)})} \left( e^{Lh_j^{(m)}} - 1 \right) \left( 2h_j^{(m)} + L \left( h_j^{(m)} \right)^2 \right) \\ &\leq e^L \left( \frac{\rho_0^{(m)}}{2} + P \sum_{\ell=1}^{n_m} h_j^{(m)} \left( e^{L\|h^{(m)}\|_\infty} - 1 \right) (2 + LT) \right) \\ &\leq e^L \left( \frac{\rho_0^{(m)}}{2} + PT(2 + LT) \left( e^{L\|h^{(m)}\|_\infty} - 1 \right) \right). \end{aligned}$$

Since equations (38) and (50) hold, we have

$$\lim_{m \rightarrow \infty} E(h^{(m)}, t^{(m)}, \rho^{(m)}) = 0,$$

contradicting equation (51).

All in all we have shown that the algorithm does indeed terminate.  $\square$

## 5 Numerical results

We compare the performance of Algorithms 3 and 4 with the previous standard Algorithm 2 in two examples.

Since the exact reachable sets are - in general - not known, we adhere to our policy of measuring the quality of approximate reachable sets in terms of the a priori error bound (11), which is usually the only measure of quality at our disposal. We measure the computational complexity of Algorithms 2, 3, and 4 in terms of the number of grid points computed in calls to Algorithm 1 as in equations (26) and (27), because for all three algorithms, the time taken to determine refined discretizations is negligible compared to that required to execute Algorithm 1 as a subroutine, see Figure 1.

Example 5.2 is a non-stiff control system. Euler's scheme is known to perform well when applied in this situation, and the error bound (11) is known to be realistic. In addition, the simplicity of Example 5.2 allows us to systematically investigate the properties of all three algorithms and the cost estimator from (27).

In contrast, Example 5.3 is a fairly nonlinear and mildly stiff control system. Euler's scheme is known to struggle when applied in this situation, see [11], and the error bound (11) is pessimistic because it does not capture that local errors are reduced by error propagation by the contractive flow.

**Remark 5.1.** *We gather some technical details.*

- a) *Since the runtimes of Algorithm 1 are extremely long for finer discretizations, we designed a workaround to compare all three algorithms through a meaningful range of error tolerances, and to provide informative illustrations in Example 5.2: Due to the simplicity of inclusion (52), we can infer the actual complexity of Algorithm 1 in dimension  $d > 1$  from running a slightly modified version of Algorithm 1 in dimension  $d = 1$  with the same discretization parameters.*

*The data displayed in Figures 1-4 and Tables 1-3 associated with Example 5.2 was generated using this workaround. All data associated with Example 5.3 was generated without this workaround.*

- b) *In all numerical computations, we implement Algorithm 4 with*

$$\varepsilon_0 \approx E(h^{(0)}, t^{(0)}, \rho^{(0)}) \quad \text{and} \quad \varepsilon_{\ell+1} = \frac{1}{2}\varepsilon_\ell \quad \text{for} \quad \ell = 0, \dots, \ell_{\max} - 1,$$

*see Algorithm 4 for the definition of  $(h^{(0)}, t^{(0)}, \rho^{(0)})$ .*



We first provide a detailed study of a simple model problem inspired by the Dahlquist test equation.

**Example 5.2.** Let  $T = 1$  and  $L \in \mathbb{R}_+$ , and consider the differential inclusion in  $\mathbb{R}^d$  given by

$$\dot{x}_i \in [0.9, 1.0]Lx_i \quad \text{for } i \in \{1, \dots, d\}, \quad x(0) = \mathbb{1}_{\mathbb{R}^d}. \quad (52)$$

The exact reachable sets are

$$R^F(t) = [\exp(0.9Lt), \exp(Lt)]^d, \quad t \in [0, 1], \quad (53)$$

and we have  $d_F = d_R = d$  and  $P = Le^L$ . We omit a plot of the numerical approximations because they do not reveal anything particularly interesting.

Since the exact reachable sets (53) of system (52) are known, we measure the quality of all numerical approximations in terms of the relative error bound

$$\delta_E(h, t, \rho) := E(h, t, \rho) / \|R^F(1)\| = e^{-L} E(h, t, \rho). \quad (54)$$

The complexity of all Algorithms was inferred using the workaround mentioned in Remark 5.1.

In the following, we examine the qualitative behavior of Algorithms 2-4 when applied to system (52) with parameters

$$d = 2, \quad L = 4 \quad \text{and} \quad \delta_E = 0.0733, \quad (55)$$

which corresponds to the numerical experiments highlighted in Table 1.

Figure 1 visualizes how Algorithms 2, 3, and 4 approach the problem in different ways. Algorithm 2 calls Algorithm 1 with the cheapest uniform discretization yielding a tolerable error, and then spends an excessive amount of time solving an unnecessarily hard problem. Algorithm 3 determines a plausible discretization without any prior knowledge of the reachable sets, and then calls Algorithm 1 to solve the corresponding problem. Algorithm 4 starts with a very rough guess for the reachable sets, and then alternately refines its guess for the optimal discretization and computes the corresponding reachable sets using Algorithm 1.

The resulting time discretizations are shown in Figure 2. Algorithm 2 chooses a uniform discretization by default. Algorithm 3 chooses monotone increasing  $h_j$  to balance out the decaying factors  $e^{L(T-t_j)}$  in (14) that bound the propagation of errors. The  $h_j$  chosen by Algorithm 4 increase even

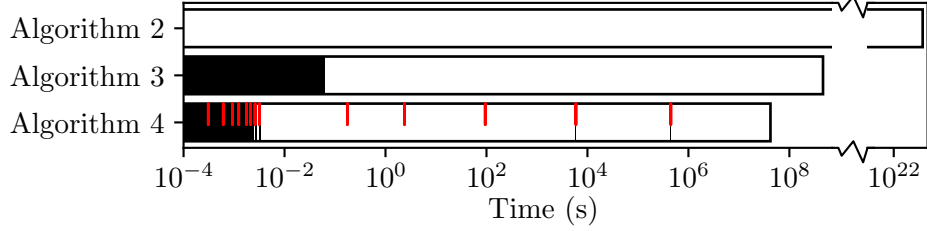


Figure 1: Complexity in terms of estimated clock time (see Remark 5.1) for system (52) with data (55). Time consumed by calls to Algorithm 1 shown in white, time spent on optimizing discretization shown in black. For Algorithm 4, the end of each call to Algorithm 1 is marked in red.

faster, because the algorithm senses that the reachable sets increase in size exponentially, and so it is much less expensive to take more steps early on.

Figure 3 shows the effect of the chosen discretizations on the cumulative normalized cost (in blue) and error (in orange) of Algorithms 2-4. The normalizations

$$[\sigma_E(h, t, \rho)]_i := \frac{1}{E(h, t, \rho)} \sum_{j=0}^i \mathcal{E}_j(h, t, \rho), \quad i = 0, \dots, n_m, \quad (56)$$

$$[\sigma_C(h, t, \rho)]_i := \frac{1}{C(h, t, \rho)} \sum_{j=0}^i \mathcal{C}_j(h, t, \rho), \quad i = 0, \dots, n_m, \quad (57)$$

help to compare the behavior of the algorithms visually.

The disparity between the local increase in error and the work invested by the algorithm is largest for Algorithm 2, and smallest for Algorithm 4. This disparity can be quantified to some degree in terms of the behavior of the algorithms in the time-interval  $[0.9, 1.0]$ : Algorithm 2 spends 82% of its entire computational budget on the interval  $[0.9, 1.0]$ , where less than 1% of the global error is generated. Algorithm 3 allocates its budget more efficiently, but still spends 61% on the interval  $[0.9, 1.0]$ , which is responsible for only 2.68% of the total error. Algorithm 4 achieves an almost perfect balance, spending 6.16% of its budget in the interval  $[0.9, 1.0]$ , which is generating 5.23% of the global error.

From now on, we test Algorithms 2-4 on inclusion (52) with several different combinations of parameters.

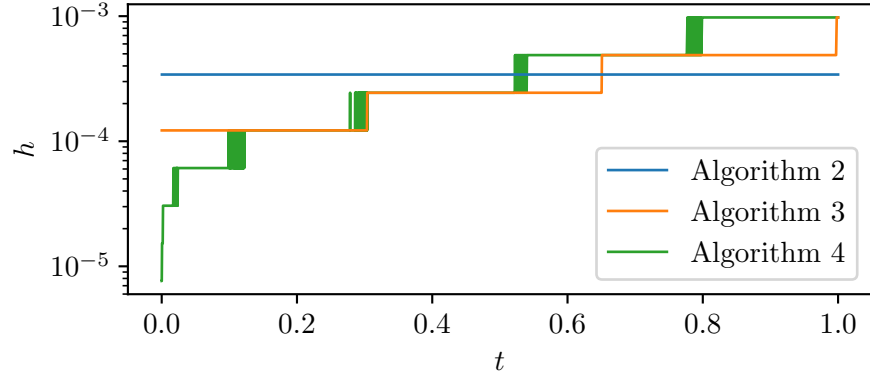


Figure 2: Final step-sizes for system (52) with parameters (55).

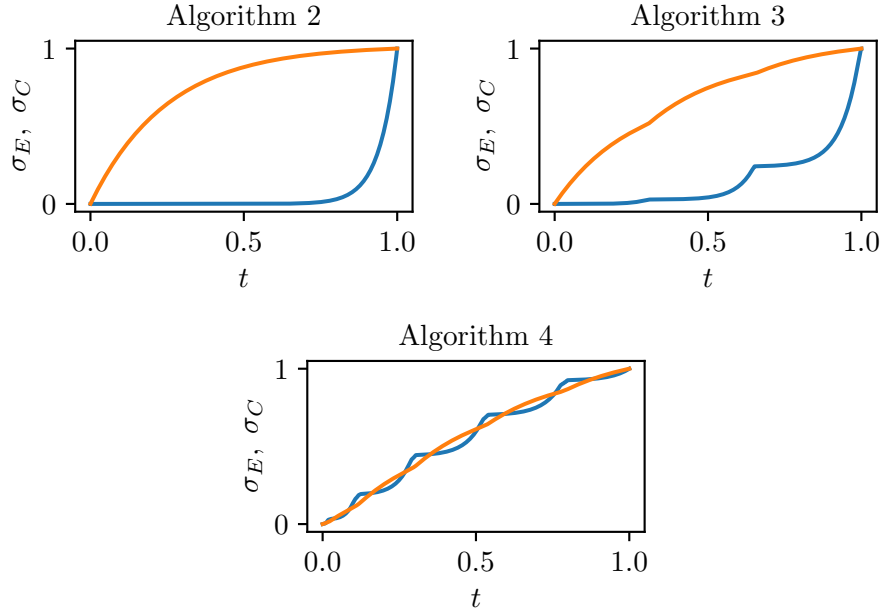


Figure 3: Cumulative contributions  $\sigma_E$  (in blue) and  $\sigma_C$  (in orange) from (56) and (57) for system (52) with parameters (55).

Table 1 shows the performance of Algorithms 2, 3, and 4 when applied to inclusion (52) with Lipschitz constants  $L = 1, 2, 3, 4$ , dimensions  $d = 1, 2$ , and several different relative error tolerances  $\delta_E > 0$ .

Algorithms 3 and 4 outperform Algorithm 2 drastically, and Algorithm 4 outperforms Algorithm 3, as expected. The differences become more pronounced for larger  $L$  and  $d$ .

Algorithm 4 is based on the cost estimator  $C$  from equations (26) and (27), which requires knowledge of the dimensions  $d_R$  and  $d_F$  of the reachable sets and the images of the mapping  $F$ . Tables 2 and 3 show how the performance of Algorithm 4 is affected when incorrect dimensions  $\tilde{d}_R$  and  $\tilde{d}_F$  are used in place of the actual dimensions  $d_R$  and  $d_F$ . The algorithm turns out to be quite robust against misjudgement, but choosing the dimensions correctly is beneficial.

In Figure 4, we study the behaviour of the estimator  $C$  by comparing its prediction to the actual cost  $\hat{C}$  incurred in the numerical experiments documented in Tables 2 and 3. Let  $(h, t, \rho) \in \mathbb{R}_{>0}^n \times \mathbb{R}^{n+1} \times \mathbb{R}_{>0}^{n+1}$ . Denoting the experimentally measured complexity of running the  $j$ -th step of Algorithm 1 by  $\hat{C}_j(h, t, \rho)$ , we define the total actual complexity and the relative error by

$$\hat{C}(h, t, \rho) := \sum_{j=0}^{n-1} \hat{C}_j(h, t, \rho), \quad (58)$$

$$\delta_C(h, t, \rho) := \frac{1}{\hat{C}(h, t, \rho)} \sum_{j=0}^{n-1} \left| C_j(h, t, \rho) - \hat{C}_j(h, t, \rho) \right|. \quad (59)$$

For every experiment with Algorithm 4 in Tables 2 and 3, we plot the relative error  $\delta_C$  of the cost estimator against the relative error bound  $\delta_E$  from equation (54) into the corresponding panel in Figure 4. Every curve represents one experiment with Algorithm 4 for a particular parameter  $L \in \{1, 2, 3, 4\}$ , and every data point represents one call of Algorithm 1 by Algorithm 4. When the dimensions  $d_R$  and  $d_F$  are chosen correctly (panels with  $d_R = d_F = \tilde{d} = 1$  and  $d_R = d_F = \tilde{d} = 2$ ), we see that

$$\lim_{m \rightarrow \infty} \delta_C(h^{(m)}, t^{(m)}, \rho^{(m)}) = \lim_{m \rightarrow \infty} \delta_E(h^{(m)}, t^{(m)}, \rho^{(m)}) = 0,$$

which confirms that the estimator is designed appropriately.

Now we consider a more complex control system from biochemistry.

$L = 1$	Algorithm 2		Algorithm 3		Algorithm 4	
$\delta_E$	$d = 1$	$d = 2$	$d = 1$	$d = 2$	$d = 1$	$d = 2$
<b>4.60E-2</b>	8.28E04	2.84E08	1.96E04	7.51E06	1.94E04	6.16E06
<b>2.30E-2</b>	1.24E06	3.27E10	2.62E05	7.11E08	2.50E05	5.47E08
<b>1.15E-2</b>	1.97E07	4.13E12	3.77E06	7.64E10	3.58E06	5.69E10
<b>5.75E-3</b>	3.10E08	5.14E14	5.73E07	8.99E12	5.42E07	6.61E12
<b>2.87E-3</b>	4.93E09	6.49E16	8.90E08	1.10E15	8.46E08	7.99E14

$L = 2$	Algorithm 2		Algorithm 3		Algorithm 4	
$\delta_E$	$d = 1$	$d = 2$	$d = 1$	$d = 2$	$d = 1$	$d = 2$
<b>1.35E-1</b>	2.91E07	2.31E13	6.08E04	3.72E07	4.96E04	1.75E07
<b>6.77E-2</b>	4.71E08	3.05E15	7.77E05	3.27E09	6.14E05	1.41E09
<b>3.38E-2</b>	7.59E09	3.97E17	1.12E07	3.54E11	8.66E06	1.36E11
<b>1.69E-2</b>	1.22E11	5.13E19	1.68E08	4.10E13	1.28E08	1.51E13
<b>8.46E-3</b>	1.95E12	6.59E21	2.60E09	4.98E15	1.97E09	1.80E15

$L = 3$	Algorithm 2		Algorithm 3		Algorithm 4	
$\delta_E$	$d = 1$	$d = 2$	$d = 1$	$d = 2$	$d = 1$	$d = 2$
<b>3.98E-1</b>	1.59E09	6.12E16	3.73E04	1.04E07	2.86E04	3.86E06
<b>1.99E-1</b>	2.63E10	8.38E18	4.37E05	7.90E08	3.26E05	2.76E08
<b>9.96E-2</b>	4.27E11	1.11E21	5.77E06	7.38E10	4.19E06	2.30E10
<b>4.98E-2</b>	6.91E12	1.46E23	8.25E07	7.88E12	5.79E07	2.24E12
<b>2.49E-2</b>	1.11E14	1.88E25	1.25E09	9.25E14	8.59E08	2.47E14

$L = 4$	Algorithm 2		Algorithm 3		Algorithm 4	
$\delta_E$	$d = 1$	$d = 2$	$d = 1$	$d = 2$	$d = 1$	$d = 2$
<b>1.17E0</b>	3.82E10	3.49E19	1.58E04	1.72E06	1.15E04	6.64E05
<b>5.86E-1</b>	6.39E11	4.92E21	1.95E05	1.53E08	1.07E05	2.77E07
<b>2.93E-1</b>	1.05E13	6.62E23	2.30E06	1.27E10	1.21E06	1.75E09
<b>1.47E-1</b>	1.69E14	8.69E25	3.06E07	1.25E12	1.52E07	1.33E11
<b>7.33E-2</b>	2.73E15	1.13E28	4.43E08	1.40E14	2.08E08	1.26E13

Table 1: Number of grid points computed by Algorithms 2-4 (see Remark 5.1) to achieve relative error tolerance (54) when applied to system (52). Colored experiments correspond to data shown in Figures 1, 2 and 3.

$L = 1$

$\delta_E$	$\tilde{d}_R = \tilde{d}_F = 1$	$\tilde{d}_R = \tilde{d}_F = 2$	$\tilde{d}_R = \tilde{d}_F = 3$	$\tilde{d}_R = \tilde{d}_F = 4$
<b>4.60E-2</b>	1.94E04	1.88E04	1.93E04	1.93E04
<b>2.30E-2</b>	2.50E05	2.61E05	2.63E05	2.63E05
<b>1.15E-2</b>	3.58E06	3.76E06	3.83E06	3.83E06
<b>5.75E-3</b>	5.42E07	5.73E07	5.82E07	5.82E07
<b>2.87E-3</b>	8.46E08	8.91E08	9.07E08	9.07E08

$L = 2$

$\delta_E$	$\tilde{d}_R = \tilde{d}_F = 1$	$\tilde{d}_R = \tilde{d}_F = 2$	$\tilde{d}_R = \tilde{d}_F = 3$	$\tilde{d}_R = \tilde{d}_F = 4$
<b>1.33E-1</b>	4.96E04	5.70E04	5.77E04	5.95E04
<b>6.77E-2</b>	6.14E05	7.04E05	7.44E05	7.78E05
<b>3.38E-2</b>	8.66E06	9.65E06	1.04E07	1.10E07
<b>1.69E-2</b>	1.28E08	1.40E08	1.55E08	1.65E08
<b>8.46E-3</b>	1.97E09	2.15E09	2.37E09	2.54E09

$L = 3$

$\delta_E$	$\tilde{d}_R = \tilde{d}_F = 1$	$\tilde{d}_R = \tilde{d}_F = 2$	$\tilde{d}_R = \tilde{d}_F = 3$	$\tilde{d}_R = \tilde{d}_F = 4$
<b>7.97E-1</b>	2.61E03	3.43E03	3.10E03	3.00E03
<b>3.98E-1</b>	2.86E04	4.13E04	4.02E04	3.24E04
<b>1.99E-1</b>	3.26E05	4.19E05	4.41E05	3.54E05
<b>9.96E-2</b>	4.19E06	5.34E06	5.75E06	4.55E06
<b>4.98E-2</b>	5.79E07	7.50E07	8.13E07	6.40E07

$L = 4$

$\delta_E$	$\tilde{d}_R = \tilde{d}_F = 1$	$\tilde{d}_R = \tilde{d}_F = 2$	$\tilde{d}_R = \tilde{d}_F = 3$	$\tilde{d}_R = \tilde{d}_F = 4$
<b>2.34E0</b>	1.77E03	1.77E03	1.77E03	1.46E03
<b>1.17E0</b>	1.15E04	1.48E04	1.58E04	1.54E04
<b>5.86E-1</b>	1.07E05	1.23E05	1.93E05	1.87E05
<b>2.93E-1</b>	1.21E06	1.32E06	1.94E06	2.04E06
<b>1.47E-1</b>	1.52E07	1.63E07	2.38E07	2.73E07

Table 2: Number of grid points computed by Algorithm 4 to achieve relative error tolerance (54) when applied to system (52) in dimension  $d_R = d_F = 1$ , using dimensions  $\tilde{d}_R$  and  $\tilde{d}_F$  in place of  $d_R$  and  $d_F$  in estimator (27).

$L = 1$

$\delta_E$	$\tilde{d}_R = \tilde{d}_F = 1$	$\tilde{d}_R = \tilde{d}_F = 2$	$\tilde{d}_R = \tilde{d}_F = 3$	$\tilde{d}_R = \tilde{d}_F = 4$
<b>4.60E-2</b>	7.43E06	6.16E06	6.39E06	7.34E06
<b>2.30E-2</b>	6.69E08	5.47E08	5.96E08	6.02E08
<b>1.15E-2</b>	8.46E10	5.69E10	6.28E10	6.41E10
<b>5.75E-3</b>	8.77E12	6.61E12	7.18E12	7.53E12
<b>2.87E-3</b>	1.27E15	7.99E14	8.71E14	9.18E14

$L = 2$

$\delta_E$	$\tilde{d}_R = \tilde{d}_F = 1$	$\tilde{d}_R = \tilde{d}_F = 2$	$\tilde{d}_R = \tilde{d}_F = 3$	$\tilde{d}_R = \tilde{d}_F = 4$
<b>1.33E-1</b>	2.12E07	1.75E07	1.94E07	2.64E07
<b>6.77E-2</b>	1.72E09	1.41E09	1.56E09	2.13E09
<b>3.38E-2</b>	2.06E11	1.36E11	1.59E11	2.01E11
<b>1.69E-2</b>	2.06E13	1.51E13	1.74E13	2.19E13
<b>8.46E-3</b>	2.94E15	1.80E15	2.06E15	2.58E15

$L = 3$

$\delta_E$	$\tilde{d}_R = \tilde{d}_F = 1$	$\tilde{d}_R = \tilde{d}_F = 2$	$\tilde{d}_R = \tilde{d}_F = 3$	$\tilde{d}_R = \tilde{d}_F = 4$
<b>7.97E-1</b>	1.83E05	1.53E05	1.17E05	1.10E05
<b>3.98E-1</b>	5.76E06	3.86E06	6.44E06	5.91E06
<b>1.99E-1</b>	3.50E08	2.76E08	3.83E08	3.38E08
<b>9.96E-2</b>	2.96E10	2.30E10	3.10E10	2.76E10
<b>4.98E-2</b>	3.01E12	2.24E12	2.76E12	2.79E12

$L = 4$

$\delta_E$	$\tilde{d}_R = \tilde{d}_F = 1$	$\tilde{d}_R = \tilde{d}_F = 2$	$\tilde{d}_R = \tilde{d}_F = 3$	$\tilde{d}_R = \tilde{d}_F = 4$
<b>2.34E0</b>	5.18E04	5.18E04	4.55E05	1.25E06
<b>1.17E0</b>	3.37E06	6.64E05	3.16E07	3.27E07
<b>5.86E-1</b>	2.65E07	2.77E07	1.91E09	2.25E09
<b>2.93E-1</b>	3.56E09	1.75E09	1.46E11	1.69E11
<b>1.47E-1</b>	1.74E11	1.33E11	1.40E13	1.66E13

Table 3: Number of grid points computed by Alorithm 4 to achieve relative error tolerance (54) when applied to system (52) in dimension  $d_R = d_F = 2$ , using dimensions  $\tilde{d}_R$  and  $\tilde{d}_F$  in place of  $d_R$  and  $d_F$  in estimator (27).

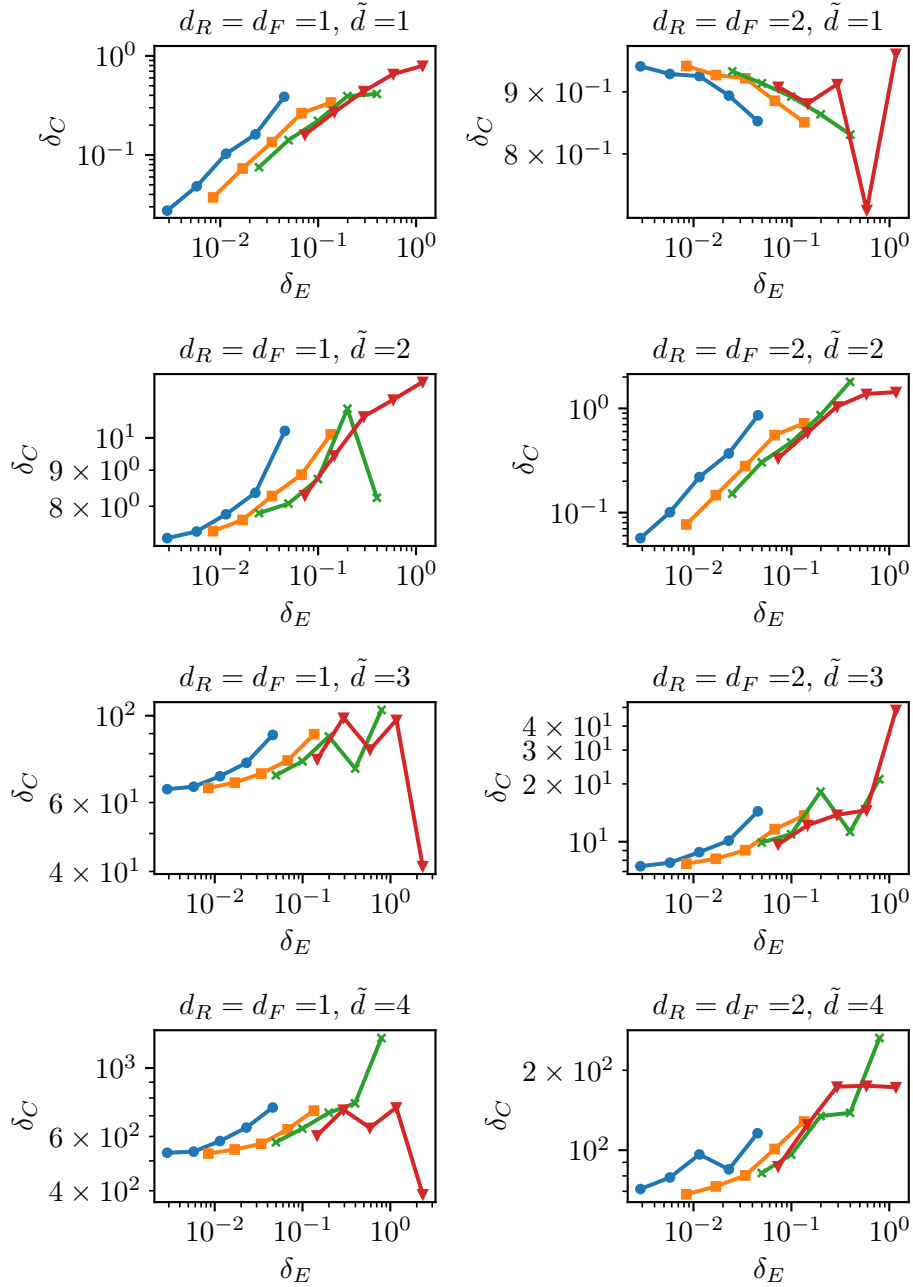


Figure 4: Relative error  $\delta_C$  from (59) plotted against relative error  $\delta_E$  from (54) when Algorithm 4 is applied to system (52). Curves for  $L = 1, 2, 3, 4$  shown in blue, orange, green, and red, respectively.



**Example 5.3.** We consider the reduced Michaelis-Menten system

$$\begin{aligned}\dot{x}_1 &= -k_1 e_0 x_1 + (k_1 x_1 + k_{-1}) x_2, \\ \dot{x}_2 &\in k_1 e_0 x_1 - (k_1 x_1 + k_{-1} + [k_2^-, k_2^+]) x_2\end{aligned}\tag{60}$$

with parameters  $e_0 = 0.6$ ,  $k_{-1} = 0.05$  and  $k_1 = 0.5$ , with an uncertainty specified by the parameters  $k_2^- = 1.8$  and  $k_2^+ = 2.0$ , and with initial conditions  $x_1(0) = 0.75$  and  $x_2(0) = 0.25$  on the time-interval  $[0, 1]$ . Note that

$$d_R = 2 \neq 1 = d_F.$$

Since the exact reachable sets of problem (60) are not available, relative error bounds as in (54) cannot be specified, and all error bounds will be provided in absolute terms.

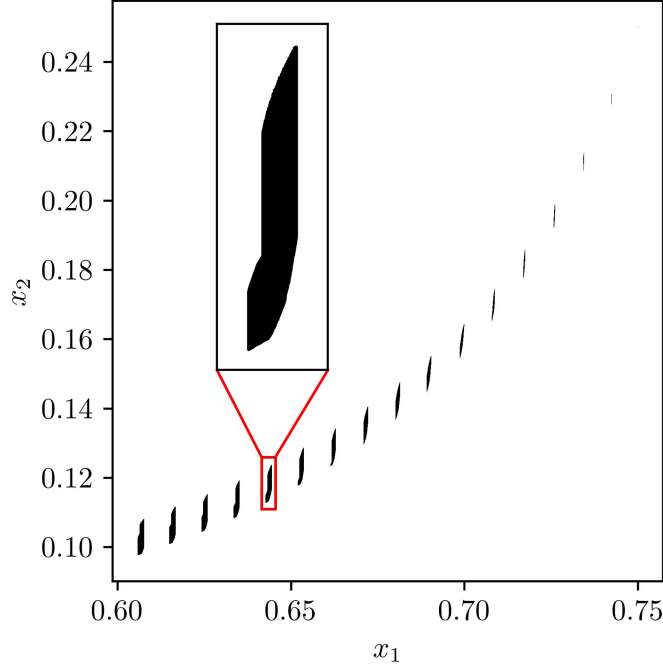


Figure 5: Approximate reachable sets of system (60) generated by Algorithm 4 with  $\varepsilon = 0.03125$ .

In the following, we examine the qualitative behavior of Algorithms 2-4 when applied to system (60) with error tolerance  $\varepsilon = 0.03125$ , which corresponds to the numerical experiments highlighted in Table 4.

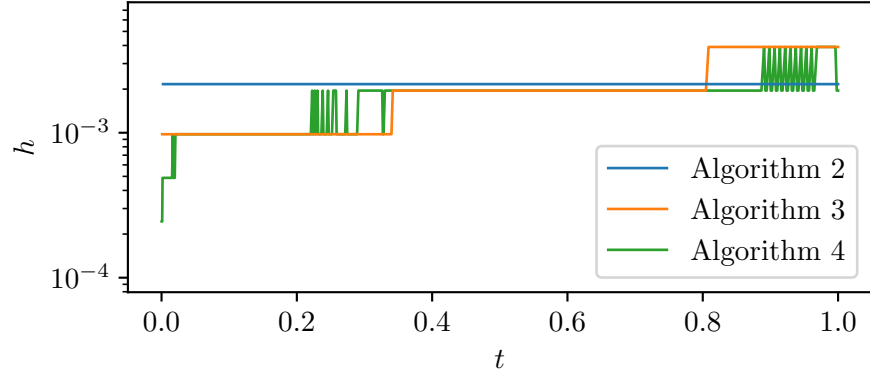


Figure 6: Stepsizes for system (60) with  $\varepsilon = 0.03125$ .

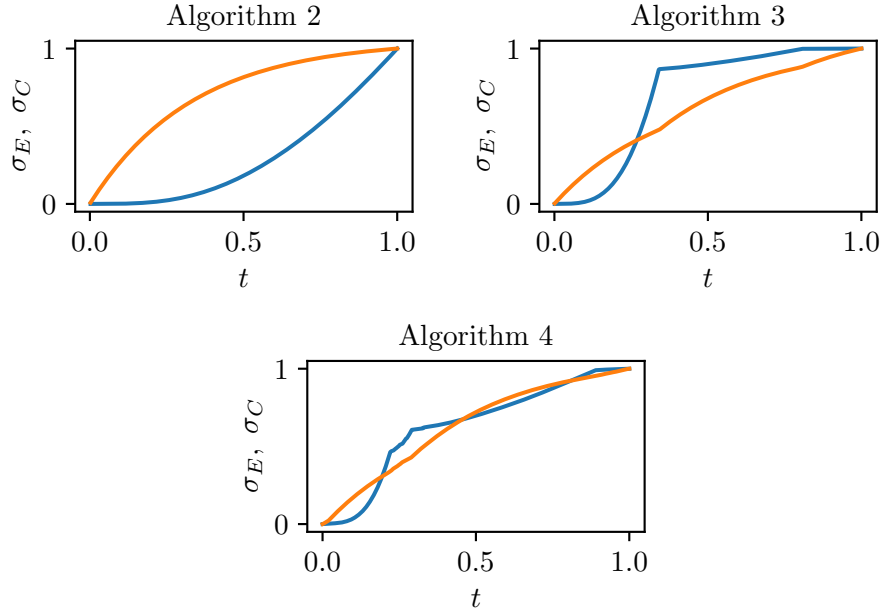


Figure 7: Cumulative contributions  $\sigma_E$  (in blue) and  $\sigma_C$  (in orange) from (56) and (57) for system (60) with  $\varepsilon = 0.03125$ .

$\varepsilon$	Algorithm 2	Algorithm 3	Algorithm 4
<b>0.25</b>	1.97E4	7.60E3	6.55E3
<b>0.125</b>	7.77E5	1.65E5	9.59E4
<b>0.0625</b>	3.33E7	7.14E6	4.87E6
<b>0.03125</b>	1.89E9	3.28E8	1.63E8

Table 4: Number of grid points computed by Algorithms 2-4 to achieve error tolerance  $\varepsilon$  for system (60).

Figure 5 shows the evolution of the approximate reachable sets generated by Algorithm 4. The sets, progressing from the top right corner to the bottom left corner of the figure, are snapshots of the reachable set taken at times  $t \in \{\frac{j}{16} : 0 \leq j \leq 16\}$ .

Figure 6 shows the time discretizations returned by Algorithms 2-4. The results are similar to those from Example 5.2 shown in Figure 2. However, since the reachable sets do not vary as much in size as in Example 5.2, Algorithm 4 cannot capitalize as much on its ability to recognize these sizes and allocate its computational budget accordingly.

Figure 7 shows the effect of these discretizations on the cumulative normalized cost (in blue, see (57)) and error (in orange, see (56)) of Algorithms 2-4. As in Example 5.2, the disparity between the local increase in error and the work invested by the algorithm to prevent the increase is largest for Algorithm 2, and smallest for Algorithm 4, but the differences are not as extreme.

Figure 8 depicts how the approximate reachable set at some fixed times  $t$  converges to the exact reachable set as the error tolerance  $\varepsilon$  decreases. Note how fine the spatial discretization has to be in order to keep the wrapping effect under control, and how this discretization drives the complexity up. In some shape or form, all numerical methods for computing reachable sets of nonlinear systems suffer from this effect.

Table 4 shows the performance of Algorithms 2, 3, and 4 when applied to system (60) for varying error tolerance  $\varepsilon$ . Again we find that Algorithm 4 is the most efficient, although the differences are less pronounced than in Example 5.2.

## 6 Discussion

In this paper, we demonstrate that the computational complexity of Euler's method for the approximation of reachable sets of control systems can be

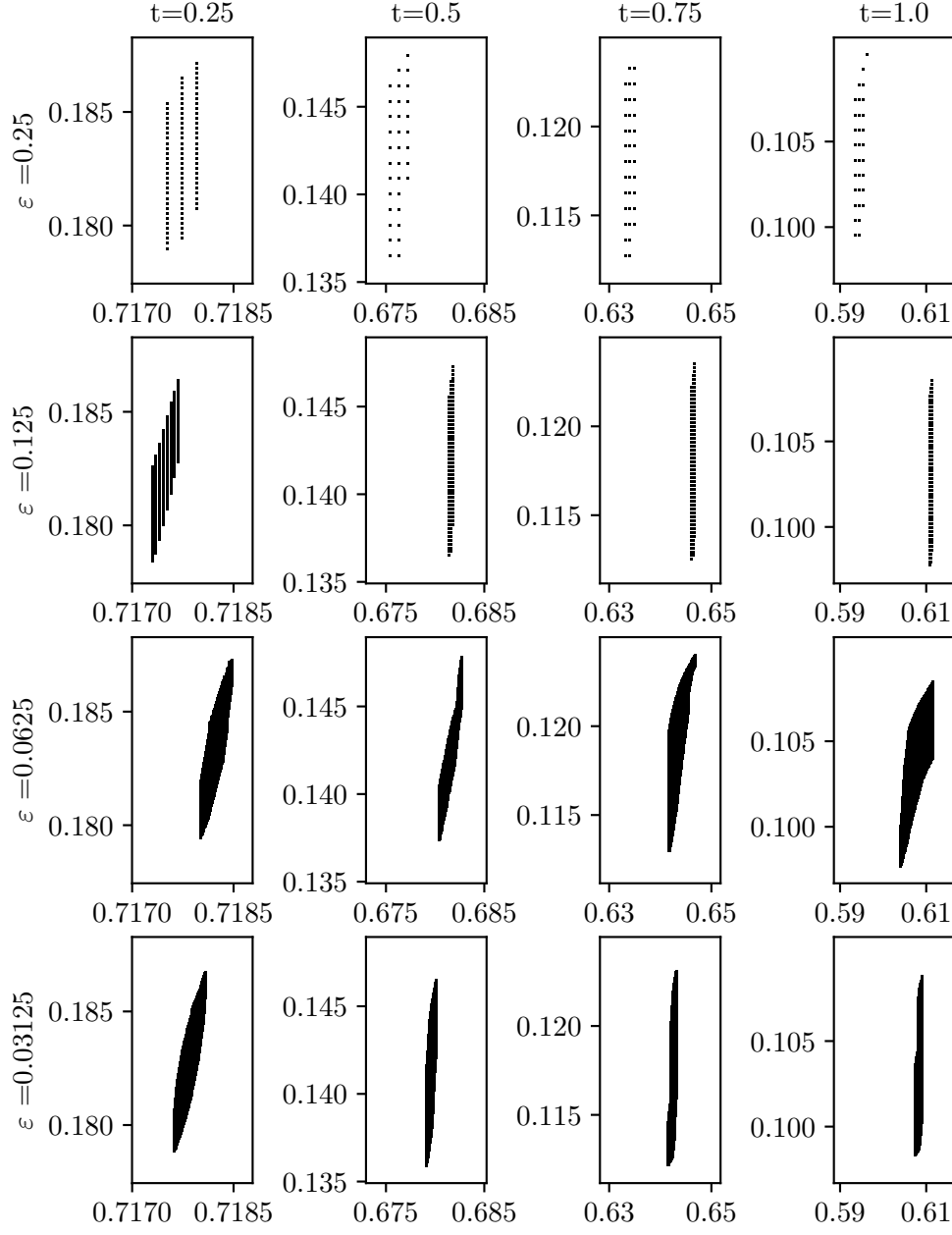


Figure 8: Approximate reachable sets of system (60) generated by Algorithm 4 for several  $t$  and  $\varepsilon$ .

reduced by using non-uniform instead of uniform space-time discretizations, and we propose two greedy algorithms that determine suitable discretizations. This raises a number of questions.

- a) In this first attempt, we have only been able to prove convergence of Algorithms 3 and 4. Is it possible to quantify their benefit over Algorithm 2 theoretically? The key challenge of this undertaking would be to quantify the dependence of the geometry of the discrete reachable sets on the discretization parameters, which may require nonstandard analytic tools.
- b) The boundary tracking algorithm from [30] computes only the boundary of the reachable sets, which reduces the computational complexity significantly. Is it possible to transfer Algorithms 3 and 4 to this setting to combine the benefits of both approaches in a single, provably convergent and highly performant algorithm?
- c) Euler's method struggles in Example 5.3, and the error bound (13) is known not to be realistic in the context of stiff systems. Is it possible to transfer Algorithms 3 and 4 to implicit and semi-implicit schemes, see e.g. [11, 26, 29], which perform well in the context of stiff systems and satisfy error bounds reflecting the qualitative behavior of these systems?

These questions may give rise to future work that is theoretically interesting and rewarding from a performance perspective.

## References

- [1] T. Alamo, J.M. Bravo, and E.F. Camacho. Guaranteed state estimation by zonotopes. *Automatica J. IFAC*, 41(6):1035–1043, 2005.
- [2] M. Althoff, O. Stursberg, and M. Buss. Reachability analysis of nonlinear systems with uncertain parameters using conservative linearization. In *Proceedings of the 47th IEEE Conference on Decision and Control*, pages 4042–4048. IEEE, 2008.
- [3] M. Althoff, O. Stursberg, and M. Buss. Computing reachable sets of hybrid systems using a combination of zonotopes and polytopes. *Nonlinear Anal. Hybrid Syst.*, 4(2):233–249, 2010.
- [4] J.-P. Aubin and A. Cellina. *Differential inclusions*, volume 264. Grundlehren der mathematischen Wissenschaften, 1984.

- [5] J.-P. Aubin and H. Frankowska. *Set-valued analysis*. Modern Birkhäuser Classics. Birkhäuser, Boston, MA, 2009.
- [6] R. Baier. Mengenwertige Integration und die diskrete Approximation erreichbarer Mengen [set-valued integration and the discrete approximation of attainable sets]. *Bayreuth. Math. Schr.*, (50), 1995. Dissertation, Universität Bayreuth, Bayreuth, 1995.
- [7] R. Baier, C. Büskens, I.A. Chahma, and M. Gerds. Approximation of reachable sets by direct solution methods for optimal control problems. *Optim. Methods Softw.*, 22(3):433–452, 2007.
- [8] R. Baier, I.A. Chahma, and F. Lempio. Stability and convergence of Euler’s method for state-constrained differential inclusions. *SIAM J. Optim.*, 18(3):1004–1026, 2007.
- [9] R. Baier, M. Gerds, and I. Xausa. Approximation of reachable sets using optimal control algorithms. *Numer. Algebra Control Optim.*, 3(3):519–548, 2013.
- [10] W.-J. Beyn and J. Rieger. Numerical fixed grid methods for differential inclusions. *Computing*, 81(1):91–106, 2007.
- [11] W.-J. Beyn and J. Rieger. The implicit euler scheme for one-sided lipschitz differential inclusions. *Discrete Contin. Dyn. Syst. Ser. B*, 14(2):409–428, 2010.
- [12] R.M. Colombo, T. Lorenz, and N. Pogodaev. On the modeling of moving populations through set evolution equations. *Discrete Contin. Dyn. Syst.*, 35(1):73–98, 2015.
- [13] R.M. Colombo and N. Pogodaev. On the control of moving sets: positive and negative confinement results. *SIAM J. Control Optim.*, 51(1):380–401, 2013.
- [14] T. Donchev and E. Farkhi. Stability and Euler approximation of one-sided Lipschitz differential inclusions. *SIAM J. Control Optim.*, 36(2):780–796, 1998.
- [15] A.L. Dontchev and E.M. Farkhi. Error estimates for discretized differential inclusions. *Computing*, 41(4):349–358, 1989.

- [16] M. Gerdtz and I. Xausa. Avoidance trajectories using reachable sets and parametric sensitivity analysis. In *System modeling and optimization*, volume 391 of *IFIP Adv. Inf. Commun. Technol.*, pages 491–500. Springer, Heidelberg, 2013.
- [17] A. Girard, C. Le Guernic, and O. Maler. Efficient computation of reachable sets of linear time-invariant systems with inputs. In *Hybrid systems: computation and control*, volume 3927 of *Lecture Notes in Comput. Sci.*, pages 257–271. Springer, Berlin, 2006.
- [18] E. Goubault and S. Putot. Robust under-approximations and application to reachability of non-linear control systems with disturbances. *IEEE Control Systems Letters*, 4(4):928–933, 2020.
- [19] L. Grüne and P. E. Kloeden. Higher order numerical schemes for affinely controlled nonlinear systems. *Numer. Math.*, 89(4):669–690, 2001.
- [20] S. Hu and N.S. Papageorgiou. *Handbook of multivalued analysis. Vol. II*, volume 500 of *Mathematics and its Applications*. Kluwer Academic Publishers, Dordrecht, 2000. Applications.
- [21] K. Knopp. *Theory and Application of Infinite Series*. Blackie And Son Limited, 1954.
- [22] N. Kochdumper and M. Althoff. Sparse polynomial zonotopes: a novel set representation for reachability analysis. *IEEE Trans. Automat. Control*, 66(9):4043–4058, 2021.
- [23] V.A. Komarov and K.È. Pevchikh. A method for the approximation of attainability sets of differential inclusions with given accuracy. *Zh. Vychisl. Mat. i Mat. Fiz.*, 31(1):153–157, 1991.
- [24] E. Lakatos and M.P.H Stumpf. Control mechanisms for stochastic biochemical systems via computation of reachable sets. *R. Soc. open sci.*, 4(8):160790, 2017.
- [25] Y. Meng, Z. Qiu, M.T.B. Waez, and C. Fan. Case studies for computing density of reachable states for safe autonomous motion planning. In *NASA Formal Methods: 14th International Symposium, NFM 2022, Pasadena, CA, USA, May 24–27, 2022, Proceedings*, pages 251–271. Springer, 2022.

- [26] B.S. Mordukhovich and Y. Tian. Implicit Euler approximation and optimization of one-sided Lipschitzian differential inclusions. In *Non-linear analysis and optimization*, volume 659 of *Contemp. Math.*, pages 165–188. Amer. Math. Soc., Providence, RI, 2016.
- [27] F. Parise, M.E. Valcher, and J. Lygeros. Computing the projected reachable set of stochastic biochemical reaction networks modeled by switched affine systems. *IEEE Trans. Automat. Control*, 63(11):3719–3734, 2018.
- [28] W. Riedl, R. Baier, and M. Gerdts. Optimization-based subdivision algorithm for reachable sets. *J. Comput. Dyn.*, 8(1):99–130, 2021.
- [29] J. Rieger. Semi-implicit euler schemes for ordinary differential inclusions. *SIAM Journal on Numerical Analysis*, 52(2):895–914, 2014.
- [30] J. Rieger. Robust boundary tracking for reachable sets of nonlinear differential inclusions. *Found. Comput. Math.*, 15(5):1129–1150, 2015.
- [31] J. Rieger. The Euler scheme for state constrained ordinary differential inclusions. *Discrete Contin. Dyn. Syst. Ser. B*, 21(8):2729–2744, 2016.
- [32] M. Rungger and M. Zamani. Accurate reachability analysis of uncertain nonlinear systems. In *Proceedings of the 21st international conference on hybrid systems: Computation and control (part of CPS week)*, pages 61–70, 2018.
- [33] M. Sandberg. Convergence of the forward euler method for non-convex differential inclusions. *SIAM Journal on Numerical Analysis*, 47(1):308–320, 2008.
- [34] M. Serry and G. Reissig. Overapproximating reachable tubes of linear time-varying systems. *IEEE Trans. Automat. Control*, 67(1):443–450, 2022.
- [35] L. Shao, F. Zhao, and Y. Cong. Approximation of convex bodies by multiple objective optimization and an application in reachable sets. *Optimization*, 67(6):783–796, 2018.
- [36] G.V. Smirnov. *Introduction to the theory of differential inclusions*, volume 41 of *Graduate Studies in Mathematics*. American Mathematical Society, Providence, RI, 2002.



- [37] V. Veliov. Second order discrete approximations to strongly convex differential inclusions. *Systems Control Lett.*, 13(3):263–269, 1989.
- [38] J. Warga. Optimal control of differential and functional equations. *New York, Academic Press, Inc.*, 1972.
- [39] A. Weber, M. Rungger, and G. Reissig. Optimized state space grids for abstractions. *IEEE Trans. Automat. Control*, 62(11):5816–5821, 2017.